MASTERARBEIT | MASTER'S THESIS

Titel | Title

Investigating the phagocytic function of innate immune cells in X-linked adrenoleukodystrophy

verfasst von | submitted by

Fanny Kormout BSc

angestrebter akademischer Grad | in partial fulfilment of the requirements for the degree of

Master of Science (MSc)

Wien | Vienna, 2024

Studienkennzahl lt. Studienblatt | Degree programme code as it appears on the student record sheet:	UA 066 834
Studienrichtung lt. Studienblatt | Degree programme as it appears on the student record sheet:	Masterstudium Molekulare Biologie
Betreut von | Supervisor:	Dr. Isabelle Weinhofer-Molisch

Table of contents

Abstract

X-linked adrenoleukodystrophy (X-ALD) is a rare neurometabolic disorder caused by mutations in the *ABCD1* gene encoding a peroxisomal ABC-transporter. The function of ABCD1 is the import of very long-chain fatty acids (VLCFAs) into peroxisomes for degradation by β-oxidation. ABCD1 deficiency leads to accumulation of VLCFAs in fluids and tissues of affected patients. X-ALD displays a striking phenotypical heterogeneity, with the default manifestation being adrenomyeloneuropathy (AMN), a slowly progressive, non-inflammatory spinal cord axonopathy. The severest form of X-ALD is cerebral ALD (CALD), a life-threatening rapidly progressive neuroinflammation characterized by disruption of the blood-brain barrier and infiltration of peripheral immune cells, culminating in demyelination and neurodegeneration. Therapeutic approaches are limited to hematopoietic stem cell transplantation or gene therapy in early stages of the disease. Cells of the innate immune system like macrophages and microglia normally expressing high amounts of ABCD1 are among the most affected immune cells in terms of VLCFA accumulation and foam cell formation, rendering them interesting targets for novel therapeutic tools. This necessitates detailed characterization of how the lack of ABCD1 impairs the function of macrophages and microglial cells. Preliminary data revealed that primary human ABCD1 deficient monocyte-derived macrophages isolated from X-ALD patients display increased phagocytic capacity compared to healthy controls. With this study, we investigated whether upregulation of phagocytosis is also intrinsic to primary murine X-ALD microglia. Using magnetic bead cell sorting, we isolated primary microglial cells from the brain of adult X-ALD and wild type control mice. After examining the purity of the isolated cells by FACS and qPCR, myelin purified from the brain of X-ALD mice and labeled with pHrodo-green, was added to the cultured cells and Incucyte Live Imaging was carried out to measure the phagocytic capacity of both genotypes. Our results revealed that X-ALD microglia showed an increased uptake of X-ALD myelin when compared to wt control cells. We were able to significantly reduce phagocytosis in both X-ALD macrophages and primary murine microglia by applying a sterically hindered oleic acid derivative (SSO), irreversibly binding to CD36, a surface receptor involved in uptake of myelin and long-chain and VLCFA. In primary murine microglia, SSO was able to normalize the uptake of myelin to wt levels. Together, our results indicate that the lack of ABCD1 in innate immune cells such as macrophages and microglia result in increased phagocytic capacity that could be normalized by application of a CD36 inhibitor. Future studies should be addressed to reveal

how the increased phagocytosis by X-ALD macrophages and microglia could contribute to neurodegenerations and neuroinflammation in X-ALD.

Zusammenfassung

X-chromosomale Adrenoleukodystrophie (X-ALD) ist eine seltene metabolische Erkrankung, deren Ursache Mutationen im *ABCD1* Gen sind, welches für einen peroxisomalen ABC-Transporter kodiert. Die Funktion von ABCD1 liegt im Import von überlangkettigen gesättigten Fettsäuren in das peroxisomale Lumen, wo diese mittels peroxisomaler beta-Oxidation abgebaut werden. Entsprechend führt ein Verlust der ABCD1 Funktion zur Anreicherung von überlangkettigen Fettsäuren in Geweben und Körperflüssigkeiten von X-ALD Patienten. X-ALD zeichnet sich durch eine klinische Heterogenität des Krankheitsbildes aus, wobei die Grundausprägung Adrenomyeloneuropathie (AMN) ist, eine langsam voranschreitende, nicht-entzündliche Rückenmarksaxonopathie. Demgegenüber steht die zerebrale X-ALD (CALD), eine lebensbedrohliche und schnell voranschreitende Entzündung des Gehirns, bei welcher die Öffnung der Bluthirnschranke zur Infiltration peripherer Immunzellen führt, welche schließlich in Demyelinisierung und Neurodegeneration endet. Bisher ist die Therapie auf hämatopoetische Stammzelltransplantation oder Gentherapie reduziert, welche nur in frühen Stadien der Erkrankung greifen.

Zellen des angeborenen Immunsystem, wie Makrophagen oder Mikroglia, welche normalerweise viel ABCD1 exprimieren, gehören zu den am stärksten betroffenen Immunzellen in Bezug auf die Anreicherung von überlangkettigen Fettsäuren, was sie zu interessanten Zielen für neue therapeutische Ansätze macht. Um dies zu bewerkstelligen ist es notwendig, exakt zu beschreiben, wie sich der Verlust von ABCD1 in Makrophagen und Mikroglia manifestiert. Aktuelle präliminäre Studien zeigen, dass primäre humane ABCD1 defiziente Makrophagen, welche aus zirkulierenden Monozyten von X-ALD Patienten differenziert wurden, ein gesteigertes phagozytisches Potential aufweisen, als jene von gesunden Menschen. Mit der vorliegenden Arbeit soll untersucht werden, ob dieses Phänomen auch bei Abcd1 defizienten Mausmikroglia besteht. Durch magnetische Trennung wurden primäre Mausmikroglia aus dem Gehirn adulter gesunder und X-ALD Mäuse isoliert und ihre Reinheit mittels FACS und RNA kontrolliert. Anschließend wurde das phagozytische Potential untersucht, indem die Aufnahme von Myelin, ebenfalls aus X-ALD Mäusen isoliert und mit pHrodo-Farbstoff gefärbt, durch die isolierten Zellen quantifiziert wurde. Durch die Quantifizierung des phagozytischen Potentials mittels “Incucyte Live Imaging” konnte festgestellt werden, dass die primären X-ALD Mausmikroglia eine höhere

Myelinaufnahme aufweisen als ihre gesunden Äquivalente. Durch den Einsatz eines CD36 Inhibitors gelang es, die erhöhte Aufnahme in sowohl humanen Makrophagen als auch Mausmikroglia zu verringern. CD36 ist eine Fettsäuretranslokase für überlangkettige Fettsäuren, welche gleichzeitig der Signalweiterleitung dient und durch ein sterisch anspruchsvolles Ölsäurederivat (SSO) irreversibel gebunden wird. Durch SSO konnte in Mausmikroglia sogar eine Reduktion auf das Niveau der gesunden Zellen erreicht werden. In Summe zeigen unsere Ergebnisse, dass der Verlust von ABCD1 in Makrophagen und Mikroglia ein erhöhtes phagozytisches Potential nach sich zieht, welches durch SSO wieder normalisiert werden kann. In weiteren Studien gilt es festzustellen, inwiefern die Erhöhung des phagozytischen Potentials zur Entstehung der Neurodegeneration und Neuroinflammation beiträgt.

Abbreviations

X-linked adrenoleukodystrophy (X-ALD)

ATP-binding cassette (ABC)

Very long-chain fatty acids (VLCFAs)

Long-chain fatty acids (LCFAs)

Adrenomyeloneuropathy (AMN)

Blood-brain barrier (BBB)

Hematopoietic stem cell transplantation (HSCT)

Scavenger receptors (SR)

Lipopolysaccharides (LPS)

Oxidized low density lipoprotein (oxLDL)

Sulfo-N-succinimidyl oleate (SSO)

Central nervous system (CNS)

ABC subfamily A1 (Abca1)

ABC subfamily D 1 (ABCD1)

ABC subfamily D 2 (ABCD2)

Cerebral adrenoleukodystrophy (CALD)

Introduction

X-linked adrenoleukodystrophy

X-linked adrenoleukodystrophy (X-ALD) is a rare metabolic, monogenic, peroxisomal disease with a combined incidence of 1:14.700 males (Yadav u. a. 2024), caused by a mutation in the gene encoding ATP-binding cassette subfamily D member 1 (ABCD1). ABCD1 is responsible for transportation of saturated very long-chain fatty acids (VLCFAs) into the peroxisome, where they undergo beta-oxidation (Turk u. a. 2020). Deficiency of the ABCD1 protein leads to the accumulation of saturated VLCFAs in tissues and body fluids where they are incorporated into various lipid classes. Lipid rich tissues like brain white matter, spinal cord and adrenal cortex are

especially affected by ABCD1 deficiency, leading to enrichment of these tissues with VLCFAs (Stephan Kemp und Wanders 2010).

To date no comprehensive model to study the pathophysiology of X-ALD has been established. At birth, patients are asymptomatic and often only develop symptoms into their thirties or forties. The youngest documented patient however was only three years old, indicating that symptoms can also occur at a younger age. ABCD1 deficiency in males causes symptoms ranging from adrenocortical insufficiency, chronic myelopathy to rapid inflammatory demyelination of cerebral white matter. Why only certain tissues are affected and what causes the diverse symptoms remains unclear (Engelen, Kemp, und Poll-The 2014).

The peroxisomal transporter ABCD1

ATP-binding cassette (ABC) transporters constitute a large superfamily consisting of 48 members, divided into subfamilies A-G. Their classification is based on structural properties as well as sequence homologies. They are localized to different parts of the cell including intracellular organelle membranes of the ER, Golgi apparatus, lysosomes and peroxisomes as well as the cellular membrane. As diverse as their localization are their ligands, ranging from lipids to nucleotides (Kawaguchi und Morita 2016).

Subfamily D consists of four members (ABCD1-4): ABCD1-3 are expressed in the peroxisomal membrane, ABCD4 is localized to the lysosomal membrane (Kawaguchi und Morita 2016). The *ABCD1* gene, located on chromosome Xq28, encodes the half transporter adrenoleukodystrophy protein (ABCD1, formerly called ALDP) that shares overlapping function and sequence homology with ABCD2 (half transporter adrenoleukodystrophy related protein, ABCD2, formerly called ALDRP) which is encoded on chromosome 12q1. The substrate specificity of ABCD1 and ABCD2 overlaps with both transporter recognizing long-chain fatty acids (LCFA) and VLCFA (C18-C26) consisting of saturated (C20:0-C26:0) and mono-unsaturated (C20:1, C22:1) fatty acids (FAs). ABCD1 however displays a higher affinity to C24:0 and C26:0 than ABCD2. In contrast, C22:6 and C24:6, highly unsaturated fatty acids, are only recognized by ABCD2. Under

physiological conditions, ABCD1 dimerizes, most likely forming homodimers, to create the functional unit of the transporter that translocates VLCFAs into the peroxisome for degradation by beta-oxidation (Stephan Kemp und Wanders 2010). ABCD3, formerly called PMP70, recognizes bile acid intermediates such as pristanic acid and phytanic acid and ABCD4, expressed in lysosomes, mediates vitamin B12 transport from the lysosome into the cytosol. ABCD1-3 recognize their respective lipid classes only as CoA-esters (Kawaguchi und Morita 2016). ABC transporter deficiencies are associated with many different disorders, such as Tangier disease (ABC subfamily A1, Abca1), cystic fibrosis (ABC subfamily C7, ABCC7) and X-ALD (ABCD1). Substrates and locations of ABCD receptors are summarized in Fig. 1.

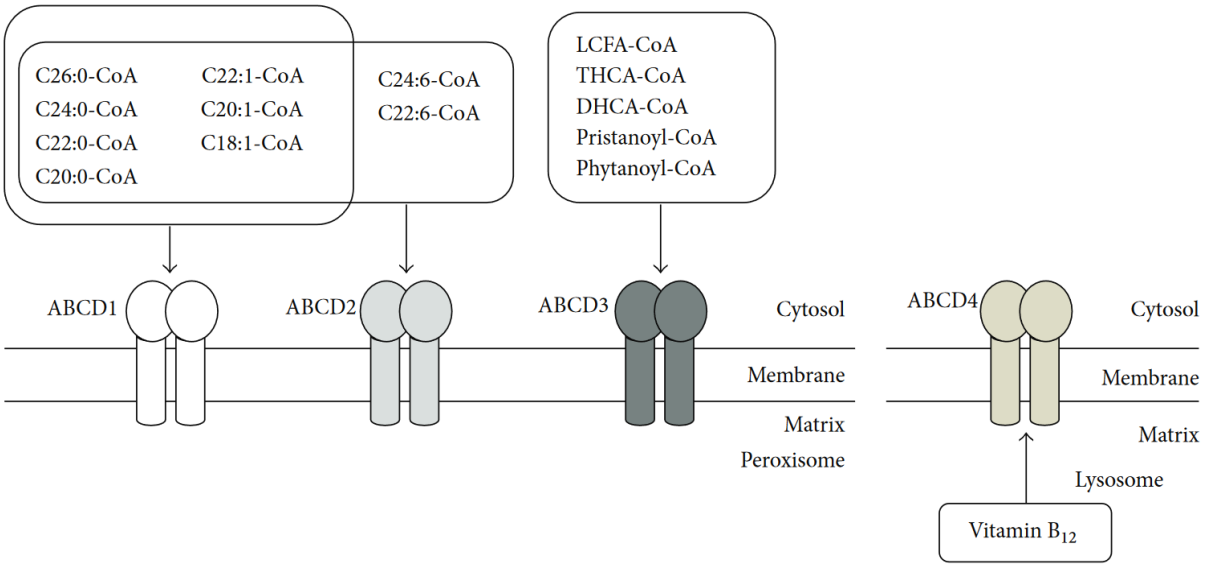

Figure 1 ***ABCD-receptors location and substrates.*** *There are 4 ABC-receptors of the subfamily D, ABCD1-4. ABCD1-3 span the peroxisomal membrane and transport different substrates into the peroxisomal lumen for degradation by beta-oxidation. ABCD1 and ABCD2 share substrates, with both recognizing mono-unsaturated C18:1-C22:1 and saturated C20:0-C26:0. ABCD2 however also transports highly unsaturated lipids such as C24:6 and C22:6. The last peroxisomal member of the ABCD subfamily is ABCD3, importing bile acid intermediates such as pristanic acid. Finally ABCD4, expressed in the lysosomal membrane, mediates B12 transport from the lysosome into the cytoplasm (Kawaguchi und Morita 2016).*

Importantly, the X-ALD phenotype, biochemically characterized by impaired peroxisomal beta-oxidation and the concomitant accumulation of VLCFAs, mainly C26:0, in body fluids and tissues of affected patients, is solely caused by ABCD1 deficiency, even though ABCD2 has been investigated as a therapeutic target against X-ALD (Pujol u. a. 2004).

Clinical phenotypes of X-ALD

Different kinds of mutations within the ABCD1 gene have been found to be related to X-ALD: missense (55.9%), frameshift (27.1%), nonsense (3.9%) and insertion/deletion mutations (3.9%) (S. Kemp u. a. 2001). However, so far no genotype-phenotype correlation could be established for X-ALD. Accordingly, despite the monogenic nature of X-ALD, the disease displays heterogeneous phenotypes that are independent of the kind of underlying ABCD1 mutation and even monozygotic twins can display different X-ALD phenotypes (Korenke u. a. 1996). The manifold of phenotypes is representative of the diversity of the affected tissues, ranging from nervous system to adrenal glands (S. Kemp u. a. 2001).

Cerebral ALD

The most severe form of X-ALD is cerebral ALD (CALD), with peak onset in boyhood between the age of 4 and 12 years (childhood CALD, CCALD, 31-35% frequency). Adult onset of CALD is less common, nevertheless, around 20% of adult X-ALD patients will also convert to CALD. The potentially genetic, epigenetic or environmental trigger that causes onset of CALD in X-ALD patients has not yet been identified (Turk u. a. 2020). CALD is a rapidly progressive neuroinflammation that is characterized by disintegration of the blood-brain barrier (BBB), infiltration of peripheral immune cells, mainly monocytes/macrophages and T cells, into the brain, resulting in demyelination and rapidly evolving extensive inflammatory white matter lesions that are characterized by a distinct zone of microglial cell death (Eichler u. a. 2008; Bergner u. a. 2019). Due to extensive demyelination and neuronal injury, CALD patients suffer from behavioral and cognitive disorders (Engelen u. a. 2012).

Adrenomyeloneuropathy

The underlying core syndrome of X-ALD with almost 100% penetrance is adrenomyeloneuropathy (AMN) that is developed by basically all X-ALD patients that reach adulthood. AMN is a slowly progressive non-inflammatory axonopathy that involves the spinal

cord and peripheral nerves. Over the course of decades, motor nerves in the lower limbs undergo atrophy, leaving arms and hands mostly unaffected. In AMN patients, brain MRI imaging seldom shows abnormalities, however if regions of increased signal intensity do occur, the small lesions are non-enhancing and non-inflammatory, thus not suffice to qualify as CALD. The spinal cord of AMN patients is characterized by non-specific atrophy, with no signs of demyelination (Engelen u. a. 2012). As outlined above, about 20% of adult AMN patients will additionally develop inflammatory CALD (Nowak u. a. 2015).

A common denominator of AMN and CALD is the frequent occurrence of Addison disease (AD), in addition to the remaining symptoms (Stephan Kemp u. a. 2016). AD is a primary adrenal insufficiency, characterized by the lack of cortisol and mineralocorticoid hormones, leading to unspecific symptoms such as fever or fatigue as well as orthostatic hypertension and anorexia. The hallmark sign of AD however is the darkening of the skin, especially in scar tissue or skin exposed to sun (Nieman und Chanco Turner 2006). About 80% of X-ALD patients develop adrenal insufficiency before adulthood. Minor symptoms include thin scalp hair and testicular insufficiencies and all X-ALD patients are asymptomatic at birth (Engelen, Kemp, und Poll-The 2014).

Female X-ALD patients rarely develop AD or CALD, however about 80 % were shown to have signs and symptoms of myelopathy after the age of 60 years, with the onset between forty and fifty years of age. About 50% of female X-ALD patients show neurological abnormalities and some symptoms are more common in female X-ALD patients, such as fecal incontinence or sensory ataxia (Engelen, Kemp, und Poll-The 2014).

Diagnosis of X-ALD

The standard testing procedure for X-ALD is the detection of VLCFA using GC-MS systems in blood samples of X-ALD patients, a reliable and reproducible, however time-consuming process (Jaspers u. a. 2020). To enable faster and more sensitive detection of VLCFA accumulation, a dried blood spot test has been established that is based on the detection of C26:0-lysophosphatidylcholine (C26:0-LPC). C26:0-LPC content is determined using LC-MS/MS, and

enables also the detection of female X-ALD patients, whose plasma VLCFA levels are normal (Jaspers u. a. 2020).

Treatment options for X-ALD

For heterozygous women or male AMN patients, only unsatisfactory treatments that are based on antioxidants or Lorenzo's oil exist (4:1 mixture of glyceroltrioleate and glyceroltrierucate (Van Geel u. a. 1999)). Trials involving Lorenzo's oil normalized plasma VLCFA levels in AMN patients, however disease progression continued. The HMG-CoA reductase inhibitor lovastatin was also able to lower plasma VLCFA levels but did not affect C26:0 levels in lymphocytes or erythrocytes and was unable to lower the content of VLCFA enriched in low-density lipoproteins (Engelen u. a. 2012). AD cause by X-ALD is treated symptomatically as it would be if it was caused by autoimmune response (Engelen, Kemp, und Poll-The 2014; Berger u. a. 2010) by treatment with physiologic replacement of the deficient glucocorticoid and mineralocorticoid hormones (Nieman und Chanco Turner 2006)

In early-stage CALD, the MRI abnormalities reflecting the progressive myelin destruction precede the onset of functional neurological deficits such as behavioral decline, visual and auditory dysfunction or gait abnormalities. This early-stage of the disease offers a critical therapeutic window where allogenic hematopoietic stem cell transplantation (HSCT) is able to successfully halt the disease progression within 6 months post treatment and leaving a mortality rate of less than 5% (Chiesa u. a. 2022), however bearing the risk of graft-versus-host-disease (Mallack u. a. 2019).

Paradoxically, induction of HSCT treatment causes a rapid progression of the disease before cessation of the symptoms, rendering it unfit to be performed on patients in more advanced stages of CALD (Chiesa u. a. 2022). Therefore, missing the early stage of CALD renders HSCT ineffective in halting CALD. This is the rational of X-ALD being included in newborn screening programs in the U.S.A., Taiwan and the Netherlands, with ongoing evaluation trials in other countries (Videbæk u. a. 2023). Next to HSCT, early-stage CALD can also be halted by gene therapy using transplantation of autologous bone marrow-derived CD34+ stem cells in vitro

corrected for ABCD1 (Biffi, Aubourg, und Cartier 2011). Even though HSCT and gene therapy are lifesaving, cognitive disabilities caused by CALD are irreversible once the damage has occurred (Turk u. a. 2020), depending on the prior symptom severity (Mallack u. a. 2019). Autologous HSCT reduces the risk of adverse immune reactions but requires prior gene therapy. Gene therapy, for somatic or germ line cells, largely relies on adenoviral or retroviral vectors and naked plasmids (Wirth, Parker, und Ylä-Herttuala 2013).

In the course of gene therapy treatment of X-ALD patients, the wild type ABCD1 gene sequence is transfected into the patient´s CD34+ stem cells ex vivo using self-inactivating lentiviral vectors, leading to the expression of functional ABCD1 in multiple CD34-derived cell types. The autologous transplant of corrected CD34+ stops disease progression (Mallack u. a. 2019). $CD34^+$ cells are released from the bone marrow and can be isolated from the umbilical cord or peripheral blood. Before transplantation, myeloablation is required to remove the resident HSCs prior to the treatment.

Both HSCT and gene therapy are able to halt the inflammatory course of early-stage CALD. However, the detailed underlying mechanisms remain unknown. It has been shown that CD34+ cells migrate into the brain and differentiate into ramified and perivascular microglia-like cells, even when the cells had been retrovirally transfected (Asheuer u. a. 2004). Thus, transfected ABCD1-reconstituted CD34+ cells, either as stem cells or CD34-derived monocytes, are able to repopulate the microglia-ablated niche, where they differentiate into microglia-like cells. (Wood 2010). In addition, CD34+ stem cells reconstitute the bone marrow, giving rise to ABCD1-corrected peripheral immune cells (Mallack u. a. 2019).

Despite great medical advancements, curative treatment is limited to early stages of X-ALD progression. The success of HSCT gene therapy shed light on the involvement of cells with hematopoietic lineage in X-ALD and raised questions about the involvement of monocytes in X-ALD pathogenesis. HSCT involving CD34+ stem cells was found to result in migration of monocyte-derived macrophages into the brain parenchyma of transplanted mice, leading to microglia senescence and the development of infiltrating macrophage-derived microglia-like cells in vivo (Sailor u. a. 2022). Accordingly, to halt CALD in X-ALD patients, replacement of the

ABCD1 deficient monocyte and microglia-lineage seems to be especially important. Of note, a previous characterization of immune cells derived from CD34+ stem cells revealed that monocytes and monocyte-derived macrophages are the immune cells most affected by the lack of ABCD1 in terms of impaired peroxisomal β-oxidation and accumulation of VLCFAs (Weber u. a. 2014). In addition, human monocyte-derived macrophages were found to display impaired plasticity to assume the anti-inflammatory state and to be pro-inflammatory skewed in X-ALD (Weinhofer u. a. 2018; Zierfuss u. a. 2022). Despite different ontogenetic heritage, both monocyte derived macrophages and microglia normally highly express ABCD1 and mediate inflammatory responses and phagocytosis of pathogens or myelin debris in both health and disease. Accordingly, understanding how the lack of ABCD1 impacts the function of X-ALD monocytes/macrophages and microglial cells is key to clarify the pathomechanism driving onset and progression of CALD in X-ALD patients.

Phagocytes

Phagocytes are immune cells that possess the ability to ingest cells or subcellular compartments and pathogens. They include bone-marrow derived cells of myeloid origin (monocytes, macrophages, dendritic cells and granulocytes) but also brain resident microglial cells. Phagocytes act along a polarization spectrum between pro-inflammatory and anti-inflammatory states allowing for appropriate responses to disturbances of tissues homeostasis while also mediating tissue repair and regeneration (Fig. 2) (Young und Denovan-Wright 2022) (Kumar 2020).

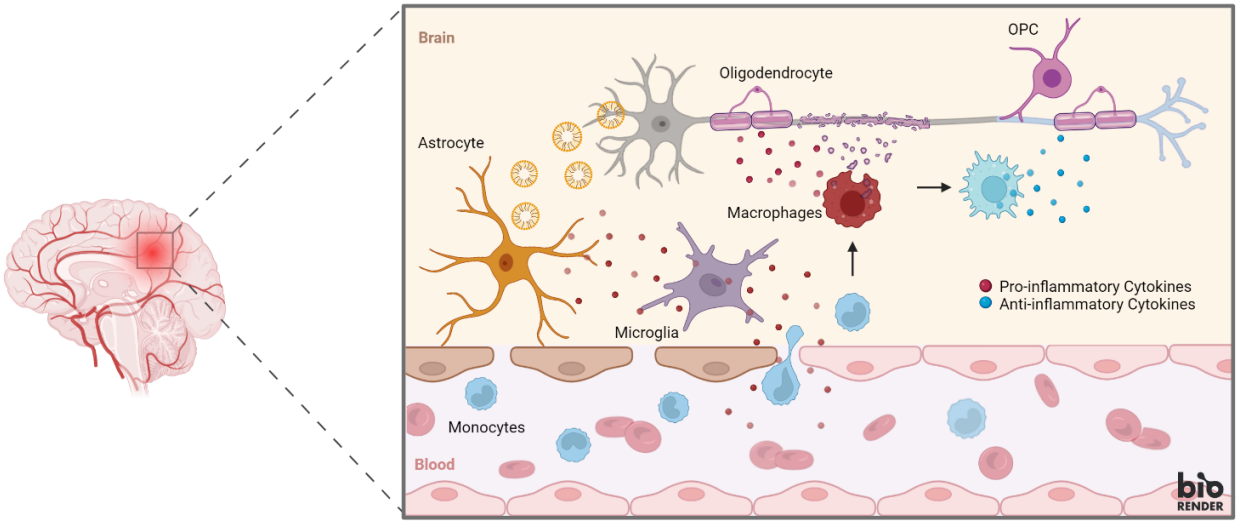

Figure 2 ***Schematic depiction of the involvement of microglia and infiltrating monocytes and monocyte-differentiated macrophages in clearance of myelin debris and subsequent regenerative function in oligodendrocyte precursor cell (OPC) recruitment.*** *Upon infection or brain injury, microglia respond by secreting pro-inflammatory cytokines (red) that cause astrocytes to loosen the BBB and to recruit peripheral immune cells such as monocytes into the central nervous system. Monocyte-differentiated macrophages and microglia clear the site of injury or infection of debris by phagocytosis. Uptake of myelin and cellular debris triggers the switch to an anti-inflammatory state, leading microglia to secrete anti-inflammatory cytokines (blue) that recruit OPCs, leading to remyelination of injured axons and regeneration of tissue. The image was generated using BioRender by Andrea Villoria-Gonzalez,M.Sc.*

Macrophages

Circulating monocytes are derived from hematopoietic stem cells in the bone marrow. Upon tissue infiltration, monocytes differentiate into macrophages (*Fig.* 3). There are three distinct subsets of human monocytes, that can be distinguished by their surface receptor pattern of CD14 and CD16: Classical ($CD14^+$, $CD16^-$), non-classical ($CD14^{dim}$,$^{CD16+}$), and intermediate monocytes ($CD14^+$,$CD16^+$) (Kapellos u. a. 2019). Scavenger receptor CD36 can serve to distinguish monocyte subpopulations (classical, intermediate, non-classical) from one another, with classic and intermediate monocytes expressing high levels of CD36, while non-classical monocytes do not express CD36 (Thomas u. a. 2017).

Even though circulating monocytes and monocyte-differentiated tissue macrophages share properties, macrophages further adapt a subset of functions specific to the tissue they are infiltrating, leading to a broad spectrum of functions, specialized for the task at hand, including but not limited to immune response and host defense. Owing to their repertoire of receptors and their ability to enter all tissues on demand, they have been referred to as an “dispersed organ

system" (Gordon und Martinez-Pomares 2017) interacting with every other bodily system. The functional path of self-replicating macrophages starts in the bone marrow where they mediate erythropoiesis and continues to the spleen and lung where they are contributing to iron recycling and surfactant homeostasis respectively. In adipose tissue they are involved in thermogenesis and insulin sensitivity in brown or white fat respectively (Gordon und Martinez-Pomares 2017). During development, macrophages influence bone remodeling by recruiting both osteoblasts and -clasts as required (Gordon und Martinez-Pomares 2017; Kumar 2020).

Macrophages mediate immune response, defending the affected tissue either by phagocytosis of pathogens or by mediating lymphocyte activation and proliferation by secretion of specific antigens (Elhelu 1983). Upon damage to the central nervous system (CNS) and concurrent release of chemotactic factors by different brain cell types, monocytes infiltrate the perivascular space and, after loosening of the BBB, further migrate into the brain parenchyma where they differentiate to macrophages. On site, macrophages help clearing myelin and cellular debris or engulf and degrade pathogens. Engulfment of lipid rich material like myelin leads to the formation of foam cells, lipid-laden macrophages; the hallmark of neurodegenerative diseases like multiple sclerosis (Grajchen u. a. 2020) and X-ALD.

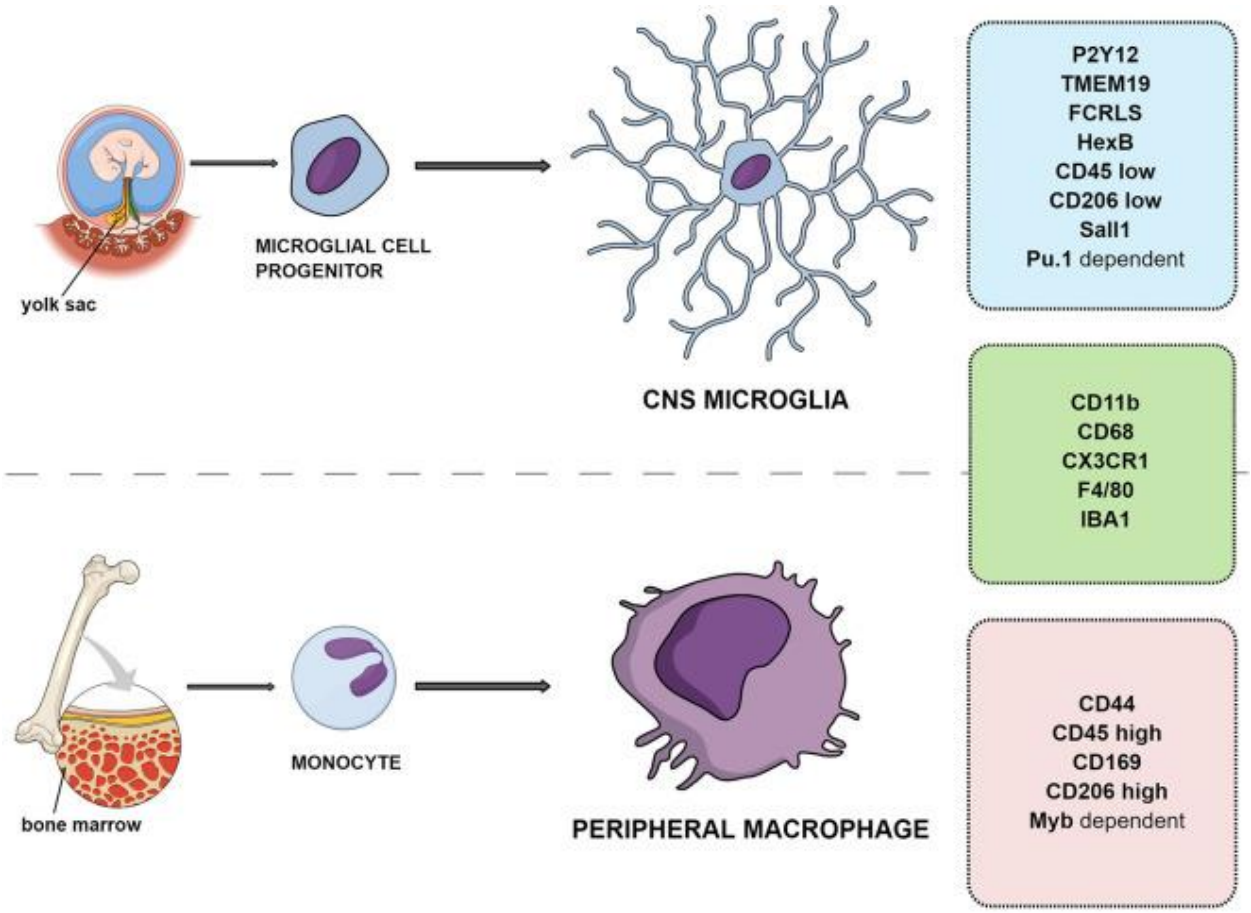

Figure 3 ***Macrophage discriminating markers in red, microglia discriminating markers in blue.*** *Markers shared by both, and other leukocytes or monocytes are shown in green. Microglia stem from the yolk-sac while macrophages differentiate upon tissue infiltration and originate from monocytes in the bone marrow (Jurga, Paleczna, und Kuter 2020).*

Microglia

As opposed to other immune cells such as macrophages or lymphocytes that are derived from the bone marrow, microglia originate in the yolk sac and differentiate to the resident innate immune cells of the central nervous system via microglia progenitor cells (Jurga, Paleczna, und Kuter 2020). They constitute about 10% - 20% of the CNS glia cell population, surveilling their surroundings as first responders to disturbance of homeostasis (Soulet und Rivest 2008) (summarized in Fig. 4). They are distinguished from other glial cell types and neurons in the brain by the expression of specific marker proteins including membrane protein cluster of differentiation 11b (CD11b) and (Ionized calcium-binding adaptor molecule 1) IBA1. CD11b and IBA1 however are not unique for microglia but are also expressed by peripheral macrophages. However, recent

research revealed markers that are highly specific for microglia such as HexB (*Fig*. 3)(Jurga, Paleczna, und Kuter 2020; Shah u. a. 2022).

Like macrophages, also microglia play a crucial role during development, by pruning synapses as well as mediating synaptogenesis by secreting neurotrophic cytokines (Sierra, Paolicelli, und Kettenmann 2019). As cells of the innate immune system, they act as first responders upon infection, secreting antiviral cytokines and factors attracting T-cells (Garden und Möller 2006). In the adult CNS upon disturbance of homeostasis including myelin destruction, microglia respond by phagocytosing myelin debris themselves and recruiting monocytes to the CNS by mediating loosening of the BBB by interacting with astrocytes. The uptake of myelin triggers the shift to anti-inflammatory response, leading microglia to secrete regenerative factors that recruit OPC or neurotrophic factors (Lloyd und Miron 2019), highlighting their dichotomous destructive/regenerative function (Fig.2).

Together, microglia and macrophages are a powerful tool to protect the brain against infection and upon injury, however pro-longed activation or impaired functions may entail pathological dystrophies as described for neurodegenerative diseases like multiple sclerosis (Van Den Bosch u. a. 2024).

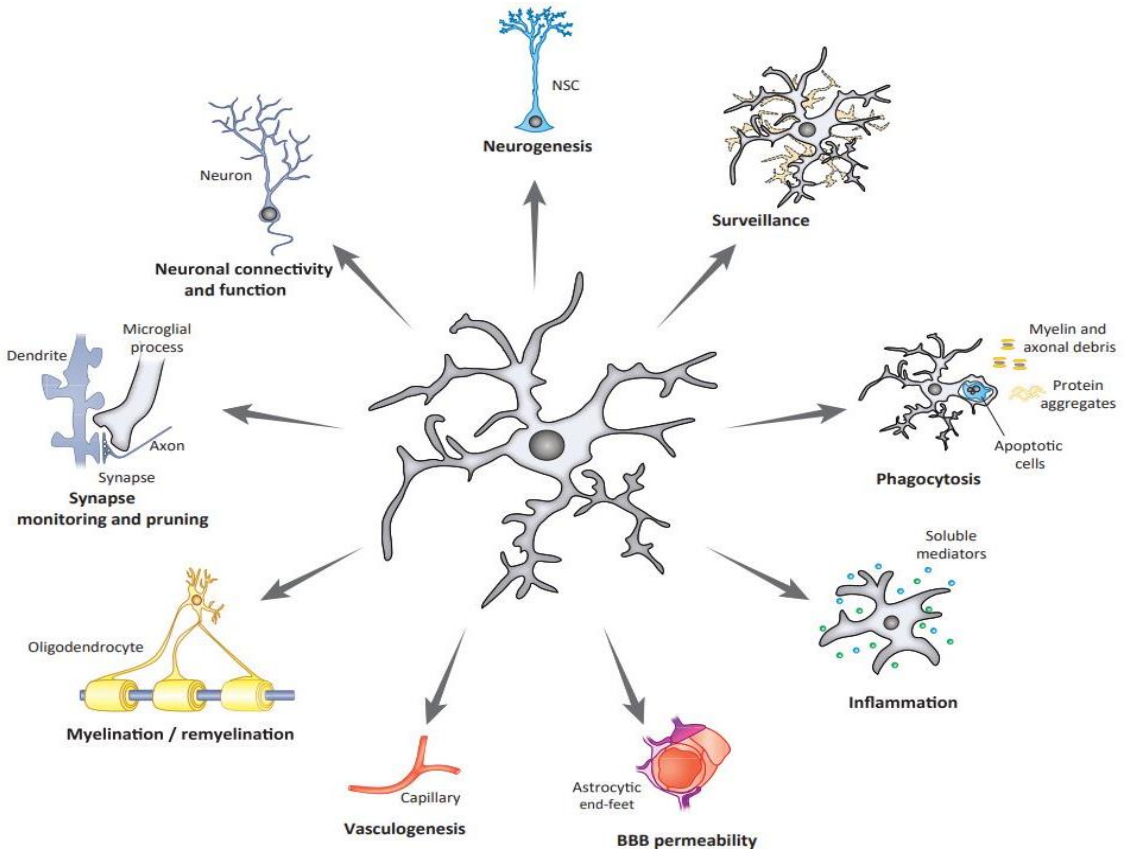

Figure 4 ***Schematic depiction of microglial function in the CNS****. Microglia support brain development and cerebral homeostasis by surveilling the brain environment and mediating immune responses to pathogens and injury through secretion of soluble mediators and phagocytosis of myelin/axonal debris, protein aggregates or apoptotic cells. They interact with other glial cell types such as astrocytes and OPCs as well as with neurons. Upon demyelination, microglia recruit OPCs to enable remyelination of neurons. Their neurogenetic capabilities make them crucial during development through pruning of synapses and the modulation of connectivity (Sierra, Paolicelli, und Kettenmann 2019).*

Both microglial cells and macrophages are phagocytic cells. Phagocytosis is defined as the recognition and engulfment of pathogens or cellular debris of at least 5 µm into plasma membrane derived vacuoles called phagosomes (Brown 1995; Botelho und Grinstein 2011). The phagosome undergoes a continuous maturation process, accumulation proton pumps and digestive enzymes, until it fuses with a pre-existing lysosome, forming the phagolysosome. Once only persistent compounds are left, hydrolase activity is maximal and the minimal pH of around 4.5 is reached,

the phagolysosome is called a lysosome (Botelho und Grinstein 2011).

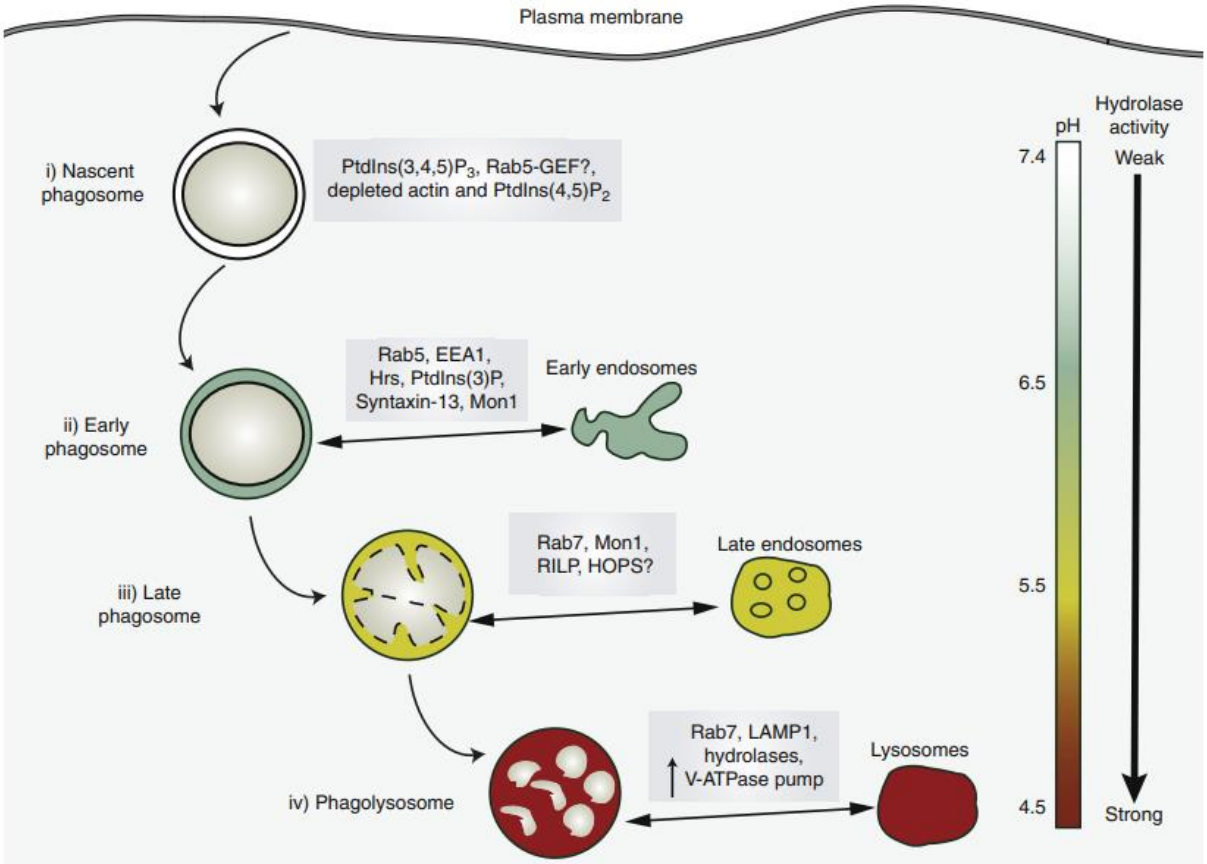

Figure 5 ***Schematic depiction of phagosome generation and subsequent fusion with the lysosome****. Upon fission from the plasma membrane mediated by phosphatidylinositol signaling, the nascent phagosome undergoes continuous fusion with endosomes, accumulating H^+-pumps and hydrolases in the maturation process from early to late phagosome. The late phagosome can undergo fission on late endosomes, sending cargo to other organelles or cells in the secretory pathway. When the phagosome fuses with the lysosome, via the phagolysosome intermediate, only persistent compounds are yet to be degraded. Finally, the phagosome has become a lysosome, characterized by maximal hydrolytic activity and minimal pH (Botelho und Grinstein 2011).*

Phagocytosis is performed by "professional phagocytes": macrophages, microglia (VanRyzin 2021), neutrophils or osteoclast among others (Gordon 2016). Recognition and uptake are mediated by a plethora of receptors and second messengers, and the destination of engulfed material varies greatly, from being circled back to the extracellular space to transport to organelles, including the lysosome, ER and Golgi apparatus.

Recognition and binding of phagocytic substrates to the cell membrane of phagocytes are receptor ligand interactions that can be opsonic, with complement or Fc receptors recognizing complement

components or antibodies, respectively. Alternatively, phagocytes can recognize particles innate properties, such as bacterial lipopolysaccharides or through so called scavenger receptors. Scavenger receptors are more promiscuous than opsonin mediated receptor-ligand interaction and recognize a broader spectrum of substrates based on biochemical properties, such as polyanionic lipids (Gordon 2016). Depending on the nature of the particle, the uptake triggers a response in the phagocyte ranging on a spectrum from pro-inflammatory to anti-inflammatory activation (Gordon 2016).

The search for putative phagocytic substrates/ligands goes beyond stochastics and is actively conducted by phagocytes. Macrophages and microglia for example sample their surroundings actively with flexible membrane extensions. Rac GTPase, phosphatidylinositol-4,5-bisphosphate (ptdIns(4,5)P2) and phosphatidylinositol-3,4,5-trisphosphate (ptdIns(3,4,5)P3) are required to form the protrusions and capture the particle. Only when receptors cluster and recognize the multivalent ligand can engulfment begin. However, the mechanism that requires multiple receptors to bind the ligand to trigger signaling is unknown. (Botelho und Grinstein 2011). Activation of non-receptor scr tyrosine kinases lead to the modification of lipids around the ligand binding area, that causes the phagocytic cup to form that in turn serves as the source for signaling: by interaction of ptdIns(4,5)P2 with the cytoskeleton, the pseudopods extend around the particle, until it is completely engulfed. Finally, the phagosome undergoes fission from the plasma membrane by myosin mediated contraction.

The aforementioned processes of membrane remodelling to enable phagocytosis render membrane properties of phagocytes interesting research subjects in X-ALD. Besides changes in the protein assembly within membranes, recent findings reveal that lipid alterations are a major factor in the initiation of phagocytosis (Saharan, Mehendale, und Kamat 2022). Sphingolipids containing saturated VLCFA ceramids were found to be enriched in phagosomes upon their formation and subsequently inhibition of ceramid synthase (CERS2), responsible for incorporation of VLCFAs into ceramides, impedes phagosome formation (Pathak u. a. 2018).

The importance of VLCFAs in phagosome formation is further consolidated by studies done in human myeloid U937 cells that identify both the enzymes responsible for elongation of very long-chain fatty acids 1 (ELOVL1) as well as CERS2 as obligatory for phagocytosis (Haney u. a. 2018).

A lack of ELOVL1 manifests as impairment of phagocytic cup formation, this phenotype however could be rescued by supplementing the lacking VLCFAs (Haney u. a. 2018).

Scavenger receptors

Scavenger receptors are transmembrane proteins that are involved in a plethora of cellular processes, including trafficking via endo- or phagocytosis or processes involved in immunity. They are expressed on microglia, macrophages, adipocytes and hepatocytes, among many other cell types. They recognize and share a broad spectrum of ligands including microbial motifs, oxidized low density lipoprotein (oxLDL), native LDL, apoptotic cells and lipids. Upon ligand binding, positive feedback mechanisms often lead to the upregulation of the involved scavenger receptor (Kelley u. a. 2014). SRs can be categorized into 12 distinct classes (A-L), based on their expression, structure and ligands.

Table 1 Overview of scavenger receptors related to the uptake of myelin debris and VLCFAs functions.

Scavenger receptor	**Function**
CD36 (SR-B3, fatty acid translocase)	Uptake: Saturared/unsaturated LCFAs/VLCFAs, oxLDL, oxidized fatty acids, phospholipids, myelin Efflux: Cholesterol (Bujold u. a. 2009)
CD 204 (SR-A1, MSR1)	Uptake: Acetyl LDL, Apolipoprotein E, apoptotic cells, oxLDL, b-amyloid, LPS

Class A SRs which include SR-A1 to SR-A6 are characterized by collagen-like domains. SR-A1, alternatively termed and subsequently referred to as CD204, recognizes LPS and lipoproteins among other ligands and is expressed on monocytes, macrophages and microglia beside a multitude of other cell types. It also acts as both signaling receptor and translocase, again mediating down-stream signaling via Nf-kB signaling and sharing translocase ligands with CD36 (Kelley u. a. 2014; Kazakova u. a. 2023).

SR-B1 to SR-B3 constitute the B scavenger class and are composed of two domains spanning the cellular membrane flanking an extracellular loop. Amino- and carboxy terminus of these receptors reach into the cytoplasm and mediate their primary functions of cholesterol and lipid transport. SR-B3, alternatively called cluster of differentiation 36 (CD36) or fatty acid translocase, will subsequently be referred to as CD36. CD36 is expressed on monocytes, macrophages and microglia and is involved in the uptake of lipids such as oxLDL and myelin (Grajchen u. a. 2020). CD36 has also been found to be responsible for the intestine's extraordinary capacity for VLCFA uptake in vivo as well as the uptake of VLCFAs in cultured cells (Drover u. a. 2008). Importantly, the CD36 mediated recognition and uptake of phagocytic substrates is linked to intracellular inflammatory signaling pathways, rendering it a receptor with dichotomous function. In CD36, ligand binding activates downstream MAP kinase, JNKs and members of the Scr family (Kazakova u. a. 2023; Kelley u. a. 2014). CD36 expression is closely intertwined with lipid metabolism, mediating lipid transport into mitochondria by interacting with mitochondrial enzyme carnityl palmitoyl transferase 1 (CPT1). Lipogenic transcription factors such as peroxisome proliferator-activated receptor γ (PPARγ) and liver X receptor (LXR) (Vogel u. a. 2022) stimulate CD36 expression, highlighting the dichotomous function of CD36 as both fatty acid translocase and signaling receptor. Despite their structural differences, CD36 and CD204 are both involved in the phagocytosis of myelin (Husemann u. a. 2002), per se making them interesting subjects of investigation in X-ALD research. Considering that accumulation of VLCFAs in X-ALD leads to their abnormal enrichment in myelin, among other lipids, renders CD36 possible importance in the context of inflammatory myelin destruction in the CALD brain. CD36 has been studied in the context of stroke induced neuroinflammation in mice, where the CD36 inhibitor Sulfo-N-succinimidyl oleate (SSO) was able to alleviate inflammatory damage to the tissue (Dhungana u. a. 2017). Sulfo-N-succinimidyl oleate (SSO) (Fig. 6) is a sterically hindered oleic acid derivative, that inhibits translocase and signaling function in CD36 but is unable to traverse the cell membrane (Kuda u. a. 2013).

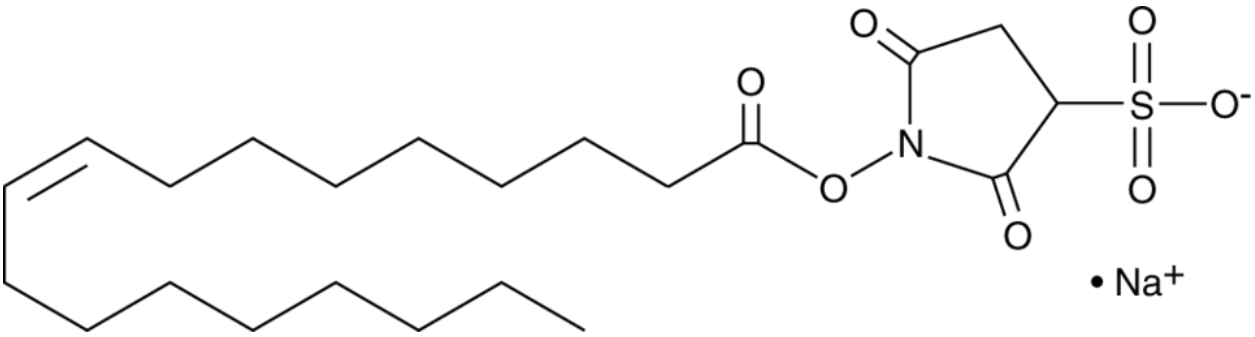

Figure 6 ***Sulfo-N-succinimidyl oleate (SSO) with sodium counterion.*** *As a sterically demanding derivative of oleic acid, SSO inhibits translocase and signaling function in CD36 by irreversibly binding the receptor. Cayman.com, 28.07.2024.*

Dosages of up to 100 µM have been described as non-toxic for human macrophages and primary murine microglia (Grajchen u. a. 2020). Other CD36 inhibitors include alkaloids like betaine or theobromine as well as flavonoids like quercetin and naringin (Feng u. a. 2022).

A class D SR is CD86, expressed on dendritic cells among others and involved in antigen presentation and T cell activation (Ohue und Nishikawa 2019). CD206 belongs to the class E SRs, is expressed on fibroblasts among others and mediated pathogen recognition (Lee u. a. 2002). A representative of class G receptors is CXCL16, a chemokine that can be expressed either as a transmembrane receptor in dendritic cells or as a soluble cytokine (Abel u. a. 2004).

Professional phagocytes play an important role in numerous neurological disorders, including Parkinson disease, multiple sclerosis, Alzheimer's disease, stroke and X-ALD. While microglia have been described as "plaque-attacking scavenger cells" (Kim und De Vellis 2005) in Alzheimer's disease, they concurrently secrete cytotoxic substances including pro-inflammatory cytokines, reactive oxygen species or proteinases, highlighting their dichotomous function (Kim und De Vellis 2005; Gong u. a. 2017).
In CALD, microglia have been found to be reduced or absent in pre-lesional brain white matter areas of chronic tissue destruction, undergoing apoptosis at higher rates than in control tissue (Gong u. a. 2017). Notably, microglial apoptosis preceded and exceeded myelin breakdown and oligodendrocyte decay (Bergner u. a. 2019). The regions bordering the lesions conversely showed a slightly activated morphology, characterized by reduced protrusion and an amoeboid shape (Bergner u. a. 2019; Kim und De Vellis 2005). The region of activated microglia was found to

overlap with regions of active inflammatory demyelination (Höftberger und Lassmann 2018) and microglia in unaffected regions of the white matter do not show increased activation patterns (Eichler u. a. 2008). The underlying reason for the loss of microglia in pre-lesional white matter has not yet been clarified but might relate to activation of cell death pathways due to increased uptake and accumulation of VLCFAs (Eichler u. a. 2008). This microglial dysfunction with subsequent cell death seems to constitute an early pathogenic change in CALD, thus possibly further contributing to continuous neuroinflammation. Elevated levels of pro-inflammatory chemokines have been observed in the cerebrospinal fluid of patients with CALD that correlate with the MRI severity of inflammatory lesions (Kim und De Vellis 2005). Phagocytes were shown to follow the edge of actively demyelinating region and are known to remove myelin debris, demonstrating that next to the brain resident microglial cells infiltrating monocytes/macrophages are key drivers in CALD. This additionally manifest as an impairment to assume an anti-inflammatory phenotype after activation and myelin removal, possibly further contributing to the prolonged inflammation in cerebral lesions (Weinhofer u. a. 2018)..

In accordance with the aforementioned hypothesis of a destructive interplay of VLCFA enriched myelin and ABCD1 deficient phagocytes, it could recently be demonstrated in our laboratory that primary ABCD1 deficient macrophages derived from monocytes isolated from the blood of X-ALD patients show increased phagocytosis of myelin isolated from X-ALD and wild type control mice (Weinhofer et al., unpublished results). Further it was found that the uptake of ALD myelin enriched in VLCFAs by healthy control macrophages is increased when compared to wild type myelin.

Aim

Despite the rarity of X-ALD, the disease represents an enormous burden for affected patients, with limited treatment options for the cerebral form and lacking interventions for AMN. As CALD is a life-threatening rapidly progressive neuroinflammation that needs to be recognized in its earliest stages in order to be halted by HSCT or gene therapy, more knowledge on the disease underlying pathomechanisms is needed to enable the development of novel treatment strategies.

The integrity of neurons is critically dependent on phagocytes that continuously survey and clear phagocytic targets throughout the entire lifespan. However, excessive phagocytosis with foam cell formation and possibly also removal of live neurons could result in pathological conditions such as neuroinflammation or neurodegeneration. Accordingly, the aim of this thesis was to use microglial cells isolated from the brain of X-ALD and control mice as well as monocyte-derived macrophages from X-ALD patients and healthy controls to assess the following research questions:

- Is the phagocytic capacity of murine X-ALD microglial cells altered when compared to wild type control cells?
- Can the phagocytic uptake by X-ALD microglial cells and macrophages be modulated by application of inhibitors targeting phagocytic receptors?

Materials and Methods

X-ALD patients and healthy controls

For monocyte isolation, peripheral blood samples were obtained from adult X-ALD patients. For isolation of monocytes from healthy controls, leukoreduction system chambers derived from male anonymous donors were purchased from the General Hospital of Vienna. The study was approved by the Ethical Committee of the Medical University of Vienna (EK1462/2014) and informed consent was obtained from X-ALD patients.

Abcd1-/y mice

The conducted work was based on *Abcd*1 deficient B6.129-Abcd1$^{tm1Kan/J}$ X-ALD mice, backcrossed on the C57BL/6J background for more than 20 generations, and wild-type C57BL/6J mice. Mice were group housed at the local animal facility of the Medical University of Vienna in an environmentally controlled room on a 12:12 h light–dark cycle and with ad libitum access to food and water.

Despite accumulation of VLCFAs in all tissues, including the brain, the ALD mouse does not develop cerebral demyelination. At around 15–16 months of age, the ALD mouse develops moderate motor deficits and neuropathologic lesions in the spinal cord that resembles AMN (Biffi, Aubourg, und Cartier 2011).

Western Blot

Buffers:

5x sample buffer
250 mM TrisHCl pH 6,8
25% (m/v) glycerol
10% SDS (w/v)
5% β-Mercaptoethanol
0.02% Bromophenol blue

1 L 10x TBST

30.2 g Tris base

87.6 g NaCl

pH 7.8

5 mL Tween

1 L 10x ELPO Running buffer (Laemmli buffer)

30.3 g Tris base

144 g Glycine

10 g SDS

1 L Blotting buffer Towbin

3.03 g Tris base

14.4 g Glycine

200 mL MeOH

1 L 5x STRIP Buffer

1 M Glycine

2.5 M NaCl

pH 2.5

Myelin isolation

Buffers:

1M Tris Cl, pH 7.45

121 g of Tris base was dissolved in 800 mL dH_2O and pH adjusted to 7.45.

Tris Cl buffer solution

To 300 mL dH_2O were added

12 mL 1M Tris Cl, pH = 7.45 at 25°C (20 mM final concentration)

2.4 mL 500 mM Na_2EDTA (2mM final concentration)

0.093 g DTT (1 mM)

Adjust pH to 7.45 and add dH_2O to 600 mL

Afterwards 2.4 mL of 25x protease inhibitor were added.

1 M Sucrose solution

To 150 mL dH_2O were added

102.69 g sucrose (1 M final concentration)

6 mL 1 M Tris Cl pH = 7.45 at 25°C (2 mM final concentration)

1.2 mL of 500 mM Na_2EDTA (2mM final concentration)

0.0465 g DTT (1 mM final concentration)

The pH was adjusted to 7.45 and dH_2O to 300 mL total volume.

Afterwards 1.2 mL of 25x protease inhibitor were added.

The 1 M stock sucrose buffer was diluted with Tris buffer to obtain 0.30 M or 0.83 M sucrose solution.

All centrifugation steps were carried out at 4°C. Before each centrifugation the tubes were balanced on a fine scale.

To purify myelin 3 whole brains were cut into pieces in 0.30 M sucrose buffer and homogenized in 7 mL total volume of the same buffer using a Dounce homogenizer (Roche), first homogenizing with 5 strokes of the loose pestle (Kontes) followed by 5 strokes of the tight pestle (Kontes).Into 6 ultra-clear tubes 6 mL of the homogenate were slowly pipetted unto 6 mL of 0.83 M sucrose buffer to perform a density gradient centrifugation in a swingout rotor (SW40Ti Beckman rotor) at 75000 g (20600 rpm) for 30 minutes with slow acceleration and deceleration. Of the three obtained phases the middle myelin layer was collected and homogenized with the tight pestle using 5 strokes in 8 mL of 0.20 M Tris Cl buffer (= Tris buffer). The combined myelin was diluted in a total of 72 mL Tris buffer and 12 mL distributed to each ultra clear tube. The tubes were centrifuged for 15 minutes at 75000 g (20600 rpm) and afterwards the supernatant was discarded. Each pellet was resuspended in 0.8 mL of Tris buffer and after homogenization in the same manner the combined myelin was diluted with Tris buffer to a total volume of 72 mL. Again 12 mL were

pipetted to the tubes and centrifuged at 12000 g (8200 rpm) for 15 minutes. The aforementioned resuspension and dilution step was repeated, and the tubes were centrifuged at 12000 g (8200 rpm) for 10 minutes.
The density gradient as well the washing steps were repeated afterwards.
Finally, the myelin pellets were resuspended in 1 mL PBS, combined and diluted in PBS to a total volume of 72 mL and centrifuged once more at 12000 g (8200 rpm) for 10 minutes. The obtained pellets were resuspended in 1 mL of PBS and stored at -20°C.

Myelin purity

10 µL purified myelin were diluted with 10 µL PBS buffer and 13.5 µL sample buffer were added. The mixture was vortexed and incubated at 55°C for 30 min in a heating block. Then the samples were vortexed again and 15 µL were loaded onto a 12% acrylamide gel for electrophoreses. The gel was run for 1 h at 60 mA. The transfer to the nitrocellulose membrane was conducted using 100 mA. Then a Ponceau stain was performed to validate the successful transfer of the protein bands to the membrane and afterwards the primary antibodies were incubated overnight. The secondary antibodies were incubated for 1 h and images were taken using chemidoc imaging system from BioRad.

BCS assay Pierce BCA Protein Assay Kit

Buffers
Reagent A
Reagent B
Working Reagent: 50:1 Reagent A:Reagent B

The following standard concentrations were diluted in 1x PBS from a 2 mg/mL bovine serum albumine (BSA) stock: 2000 µg/mL, 1500 µg/mL, 1000 µg/mL, 750 µg/mL, 500 µg/mL, 250 µg/mL, 125 µg/mL, 25 µg/mL.

Standard curve

The standards and samples were prepared and measured in the same manner. The absorbance was measured at 562 nm and a linear standard curved was fitted to the standard values with a R of 99,6%.

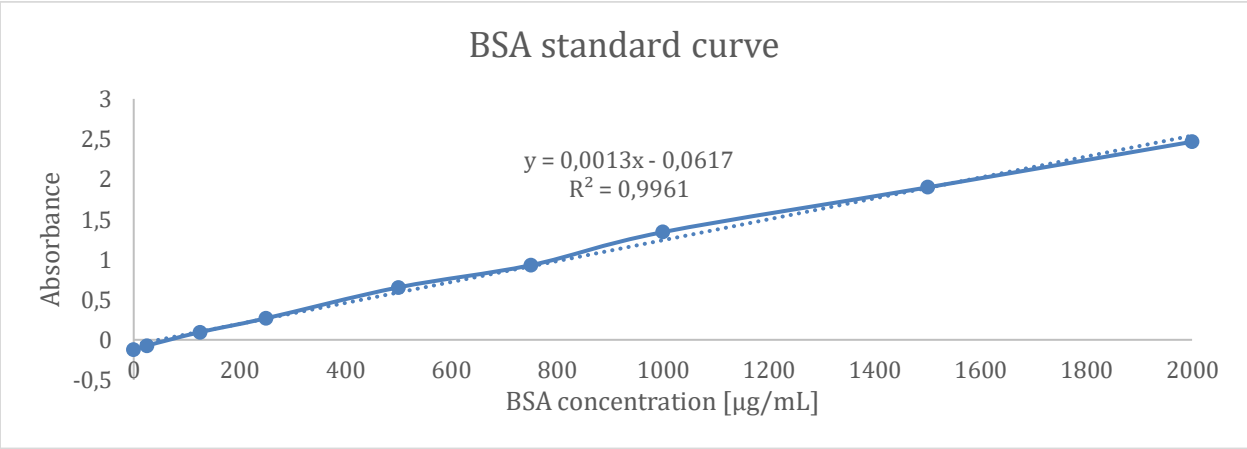

Sample preparation for test tube procedure (sample to working reagent ratio of 1:20)

Samples and standards were measured in duplicates. 100 µL of sample or standard were diluted in 2 mL of working reagent, mixed and incubated in an 37°C water bath in the dark for 30 min. 1 mL of samples or standard were measured in a cuvette at 562 nm after cooling to RT.

Endotoxin concentration determination

ToxinSensor™ Chromogenic LAL Endotoxin Assay Kit by Genscript was used to determine the endotoxin concentration in isolated myelin.

Reagents

Limilus Amoebocyte Lysate:
Chromogenic substrate
Stop solution
Color stabilizer 1 (=Buffer S)
Color stabilizers 2 and 3
Standard endotoxin solutions

100 µL of standards, samples and H_2O were pipetted into endotoxin free vials and vortexed for 30 seconds. 100 µL of LAL was added and the mixture was incubated at 37°C in a heating block for 20 minutes aber being mixed. 100 µL of chromogenic substrate were added and after mixing the reaction was incubated for 6 minutes at 37°C in a heating block. 500 µL of stop solution and color stabilizer 2 were added and mixed after each addition. 500 µL of color stabilizer 3 were added and after a final mixing the absorbance was measured at

pH Rodo labelling

0.5 mg of pHrodo dye were dissolved in 500 µL of DMSO. Isolated myelin and synaptosomes were diluted with PBS pH = 8.0 to a final concentration of 2 mg/mL of protein content and incubated with 1:1000 pHrodo dye per milligram protein for 45 minutes. The suspension was spun down (5 minutes, 4°C, 12000 g) and resuspended in PBS pH 7.4.

Microglia isolation

Enzyme mixes/buffers

Enzyme mix 1: 50 µL Enzyme P + 1.9 mL buffer Z
Enzyme mix 2: 10 µL Enzyme A + buffer Y

To isolate microglia from murine brain tissue, the Miltenyi biotech adult brain dissociation kit mouse/rat was used. The obtained cell suspension was isolated using the MiniMacs separator and columns. The brains were dissected from freshly sacrificed mice, washed in D-PBS and transferred to C tubes and cut using sterile scalpels in enzyme mix 1. Enzyme mix 2 was added and the mixture was homogenized using the gentle MACS Octo dissociator with heater at 37°C for 30 min.

The homogenate was spun down to collect the tissue suspension at the bottom of the tube and transferred to 50 mL falcon tubes by straining it through wetted (D-PBS) 70 µm smart strainers and washing with 10 mL of D-PBS. After centrifugation at 300xg for 10 min, at 4 °C, the supernatant was removed and the pellet resuspended in 1 mL of D-PBS, transferred to a 15 mL tube and filled up to 3.1 mL with D-PBS. 900 µL of debris removal solution was added and after mixing 4 mL of D-PBS were added as a second phase. After centrifugation (1000 x g, 10 minutes, 4°C) with full acceleration but no brake, the top two phases were removed, the remaining phase was diluted to 15 mL total volume using D-PBS and inverted until the pellet was dissolved. After centrifugation (1000 x g, 10 minutes, 4°C) with full acceleration and brakes the supernatant was removed and the pellet resuspended in 1 mL red blood cell removal solution. After 10 minutes of incubation at 4°C in the dark, 10 mL of PBS/FCS were added. After another centrifugation (300 x g, 4°C, 10 minutes) the supernatant was removed, and the pellet resuspended in 97.5 µL PBS/FCS and 2.5 µL vortexed O4-beads were added. After thorough mixing, the suspension was incubated at 4°C in the dark for 15 minutes. 1 mL of PBS/FCS was added and the suspension was centrifuged (300 x g, 4°C, 5 minutes). The supernatant was removed, and the pellet resuspended in 500 µL PBS/FCS. The cells were magnetically separated by applying the suspension to the column containing metallic beads placed on a magnetic stand. The flow through was collected and stored on ice and was later used to isolate further cells. The column was removed from the magnetic stand and the oligodendrocytes could be flushed out using a stamp. The flow through was centrifuged and the supernatant removed, then 90 µL FCS/PBS were added and the pellet was thoroughly dissolved before 10 µL of Anti-CD11b microbeads were added, and the procedure was repeated.

In vitro differentiation of human monocytes to macrophages

CD14+ monocytes were seeded in LPS-free RPMI medium (Sigma-Aldrich) containing 1% Penicillin/Streptomycin (Invitrogen), 1% glutamine (Invitrogen), 1% Fungizone (Invitrogen), and 10% fetal calf serum (FCS, Invitrogen), supplemented with 50 ng /mL human recombinant macrophage colony-stimulating factor (M-CSF) (PeproTech) for seven days.

Calcein AM stain

Calcein-AM red viability dye by Thermofisher was used to determine cell count in human macrophages. Calcein bound to acetoxymethyl (AM) is membrane permeable and cleaved by intracellular esterases in live cells, leaving free fluorescing Calcein (Ex: 495 nm, em: 515 nm) while dead cells give no signal.

Macrophages seeded in 96-well plates were washed with 100 µL PBS before addition of 25 nM Calcein-AM red in PBS. After 40-60 min of incubation at 37°C, 5% CO_2 pictures were taken to quantify cell counts. As negative control cells were treated with 70% EtOH before the addition of Calcein-AM.

Flow cytometry

Antibodies:
CD11b-APC
CD93-APC 5 µL
CD36-APC
CD204-PE 5µL
O4-PE
Isotype PE
Isotype APC
Isotype FITC
Mer-APC
ACSA-FITC

50.000-100.000 cells per stain were spun down (5 minutes, 300g, 4°C) and resuspended in 35 µL 10% Beriglobin in PBS and incubated for 30 minutes at 4°C in the dark. Then 1.25 µL (5 µL for CD93 and CD204) of antibodies were added per stain and incubated for 10 minutes at 4°C in the dark. The cells were spun down (5 minutes, 300g, 4°C) and resuspended in 250 µL PBS.

Receptor expression was assessed via flow cytometry using Guava® easyCyte with GuavaSoft™ software (both Merck KGaA).

Statistical analysis

GraphPad Prism version 8 was used to carry out statistics as well as to design graphs. Statistical tests were used as indicated in the figure legends. P-values below 0.05 were regarded to indicate statistical significance.

Live Imaging Phagocytic Assay

Microglia

Primary murine microglia were seeded into 96-well plates in DMEM (Sigma-Aldrich, 4.5 g/L glucose, L-glutamine, sodium pyruvate and sodium bicarbonate) supplemented with 10% FCS with M-CSF (0.2 µL in 200 µL) after isolation. The medium was renewed after 24 h and the cells were differentiated for 5 days at 37°C, 5 % CO_2 before treatment.

Cells were exposed to 10 µg/mL of X-ALD Myelin, and 20/50 µM sulfo-N-succinimidyl Oleate (SSO,Cayman, sodium salt, Item: 11211, dissolved in DMSO) and autofluorescing lipofuscin was used to quantify cells. Once the treatment was added, the cells were imaged for 48 h using Incucyte Live-Cell Analysis System SX5 (Sartorius AG) which was housed inside an incubator at 37°C and 5% CO2. Four images per well were taken every hour using a 10x objective lens and then analysed using the IncucyteTM Software. Green channel acquisition time was 300 ms and orange channel 400 ms. The green threshold of green corrected units was set based on untreated cells at timepoint zero and 24 h. The orange channel threshold was set to exclude debris and background.

Macrophages

Primary human monocytes were seeded into 96-well plates in LPS-free RPMI-1640 supplemented with 10% FCS and 50 ng/ml M-CSF in 200 µL medium and differentiated into macrophages. Media was renewed on day three and five, after seven days 20 µg/mL of Myelin/X-ALD Myelin was added. After addition of the substrate cells were imaged for 24 h using Incucyte Live-Cell Analysis System (Sartorius AG) which was housed inside an incubator at 37°C and 5% CO2. Four

images per well were taken every hour using a 10x objective lens and then analyzed using the IncucyteTM Software. Green channel acquisition time was 300 ms and orange channel 400 ms.

Results

Previous, yet unpublished studies carried out in our laboratory revealed that macrophages in vitro differentiated from monocytes isolated from the blood of X-ALD patients present with increased phagocytic capacity when compared to healthy controls. In the brain, microglial cells are the resident innate immune cells and main phagocytes, potentially linking them to CALD pathogenesis. Due to limitations in the direct accessibility of human primary microglial cells and not yet finally established differentiation protocols of induced pluripotent stem cells towards microglial cells in our lab, we set out to test whether the stronger phagocytic response of human X-ALD macrophages would also be recapitulated in primary murine microglial cells isolated from X-ALD mice.

Isolation and culture of primary microglia, from the brain of X-ALD and wildtype control mice.

To obtain primary microglial cells, brains from X-ALD and wt mice were dissected, and then homogenized mechanically and chemically to obtain a single cell suspension. The respective cells were separated using magnetic beads involving antibodies directed against Oligodendrocytes (O4) and microglia (CD11b). Upon isolation, the cell number of both microglial cells and oligodendrocytes was determined using an automated cell counter. From a single mouse brain, usually 250.00 microglia/mL were obtained and 1.8 Mil. oligondendrocytes/mL could be removed. At this point, FACS analysis to assess the purity of the obtained fractions (microglia/oligodendrocyte) was conducted from initial experiments. Remaining cells were immediately harvested for RNA isolation or microglial cells were seeded and cultivated.

To assess microglial functions such as response to a pro-inflammatory LPS stimulus or phagocytosis, isolated murine microglia were in vitro cultured for five days, with the medium being changed on the first day after isolation to remove cell debris and potential myelin contamination. Directly after isolation, the cultured microglial cells displayed an amoeboid morphology and were surrounded by cell debris, resulting from the isolation procedure. After the medium change on day 2, the amount of debris was significantly reduced but could not be removed

entirely. During the five-day period before the functional assessment of the microglia, the number of cells showing a ramified or rod-like morphology steadily increased until finally a spectrum of morphologies was present (Fig. 7). Both X-ALD and wt microglial cells displayed a similar morphological spectrum and confluence.

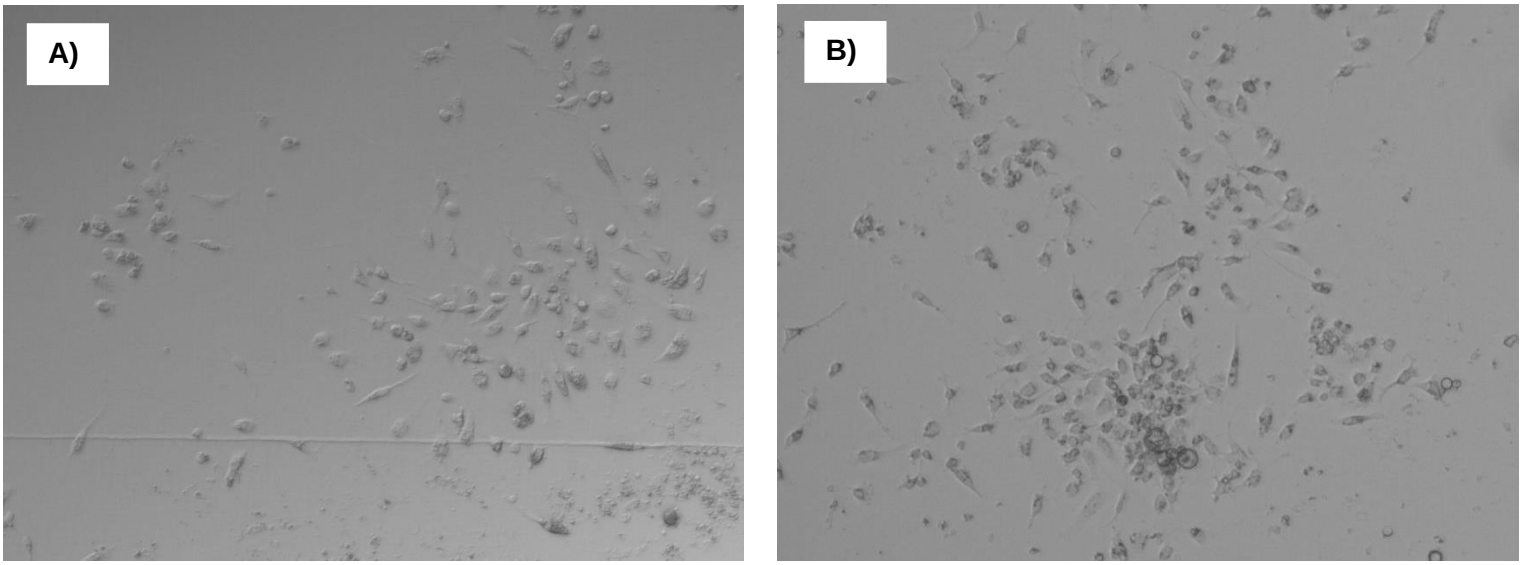

Figure 7 ***Cultivation of isolated primary murine microglial cells derived from X-ALD and control mice****. Cells were cultured for 5 days before transmission light microscopy using 40x magnification was carried out. (A) X-ALD and (B) wild type microglial cells.*

To determine the purity of the isolated cell fractions, flow cytometry using fluorescently labeled anti-mouse antibodies directed against CD36 and O4 fused to APC or PE fluorophores, respectively, were used. To control for unspecific binding of the antibodies, a stain with the respective isotype antibody (isotype-APC and isotype-PE) was included next to an unstained fraction. Each fraction was stained for the desired cell type as well as for possible contaminants. In Fig. 7, a representative picture of three independent experiments is shown where the microglia fraction purity was assessed by FACS. In this experiment, 92% of cells were found to be positive for CD11b expression (Fig.xy). When cells were stained for the astrocytic marker astrocyte cell surface antigen (ACSA), only a small proportion of 3% of the total cell population was found to be positive, indicating only a minor contamination with astrocytes. For oligodendrocytes and OPCs, the contamination was usually in the range of 5%, indicating the efficient removal of myelin.

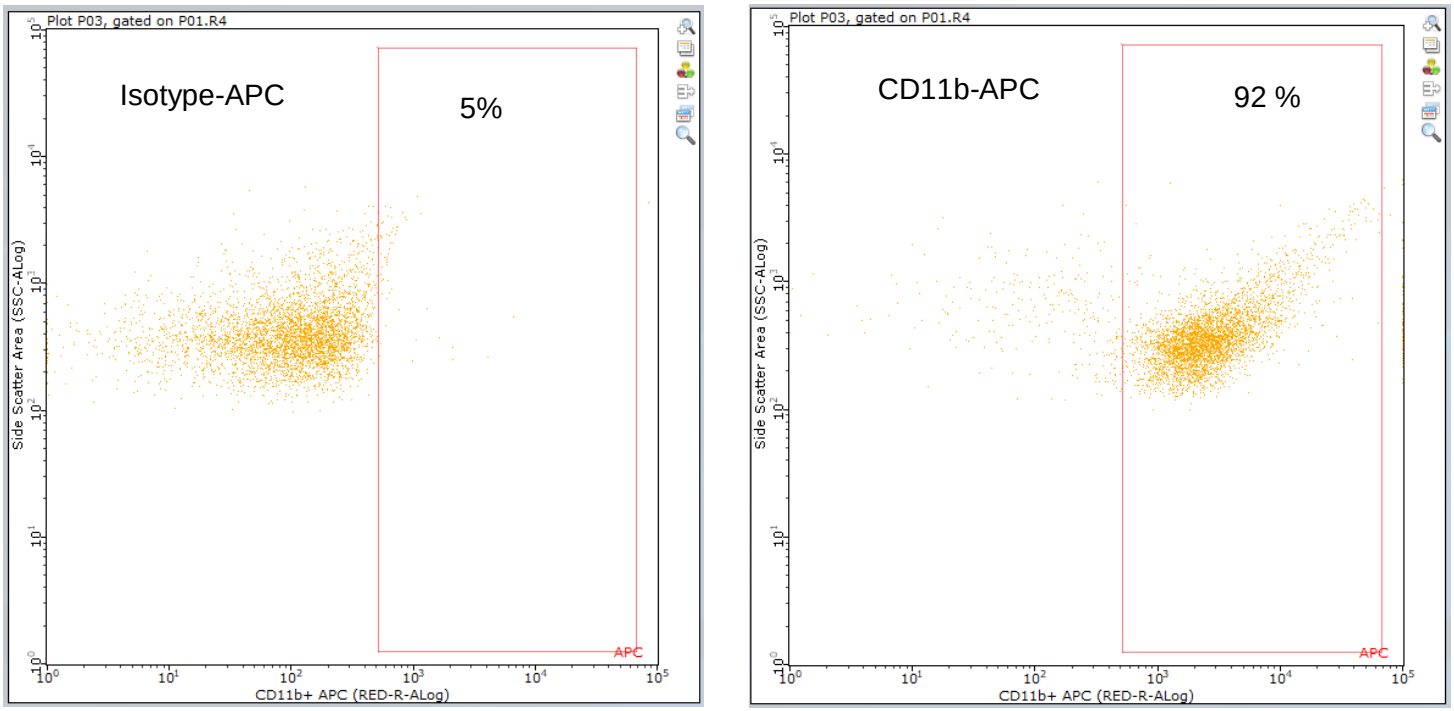

Figure 8 ***92% purity could be obtained in the microglia fraction****. The left panel shows the entirety of alive cells in the microglia fraction, quantified using the binding and APC-fluorescence of the isotype antibody. The red window on both panels marks the borders within which cells are considered microglia. Upon CD11b-APC binding fluorescence intensity shifts (right panel) allowing the quantification of microglia. Quantification of contaminants is not shown.*

In addition to verification of the purity via FACS targeting surface receptor CD11b expression, RNA analysis was conducted from microglia and oligodendrocytes isolated from the brain of three X-ALD and three wild type control mice (Fig. 9). Upon RNA isolation, cDNA was generated, and expression of the microglia and oligodendrocyte lineage marker genes ionized calcium-binding adapter molecule 1 (Iba-1) and proteolipid protein 1 (Plp1), respectively, were assessed using qRT-PCR, with normalization to expression levels of hypoxanthine-guanine phosphoribosyltransferase (HPRT).

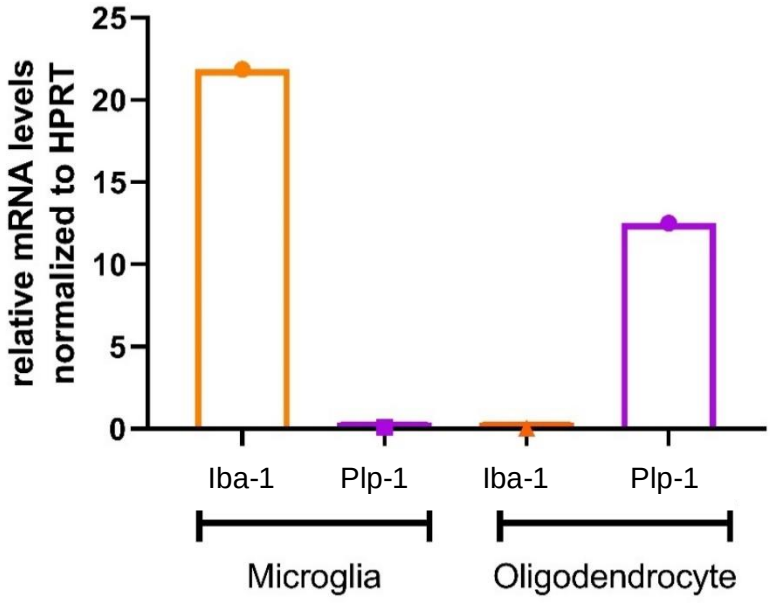

Figure 9 ***qRT-PCR analysis of microglia and oligodendrocyte fractions isolated from the murine brain confirmed the high purity of isolated cell populations.*** *Relative mRNA levels of the microglia marker Iba-1 revealed an enrichment of Iba mRNA levels in the microglia fraction when compared to isolated oligodendrocytes. Low relative expression levels of oligodendrocyte marker Plp1 confirm the negligible contamination of the microglia fraction. The inverse is true for the oligodendrocyte fraction, reveling that oligodendrocyte removal was effective. The graph represents the average outcome of 3 different experiments, fold-change is normalized to the respective marker levels in the Astrocyte positive fraction.*

Considering that X-ALD mice do not develop the CALD phenotype, the question arose whether the functionally related Abcd2 would compensate the loss of Abcd1 in murine microglial cells. To address this question, we next assessed whether the expression levels of Abcd1 and Abcd2 would differ between isolated murine microglial cells and human microglia cells differentiated from induced pluripotent stem cells (iPSC). We retrieved data on human microglial ABCD1 and ABCD2 expression from the published RNAseq data set GSE221013 (Sabogal-Guáqueta u. a. 2023) and compared the levels of gene expression to those observed from our murine microglial

cells (fig. 10). We found that both human iPSC-derived and microglia isolated from the brain of mice present with a similar ratio of ABCD1 and ABCD2 expression, potentially indicating that differences in ABCD2 expression between the species might not account for the lack of cerebral involvement in X-ALD mice.

Considering the involvement of innate immunity in the development of CALD and previously observed pro-inflammatory skewing of X-ALD macrophages (Weinhofer u. a. 2018), we next tested whether the inflammatory response is also altered in primary murine X-ALD microglia when compared to wt cells. We treated microglial cells derived from either X-ALD or wild type

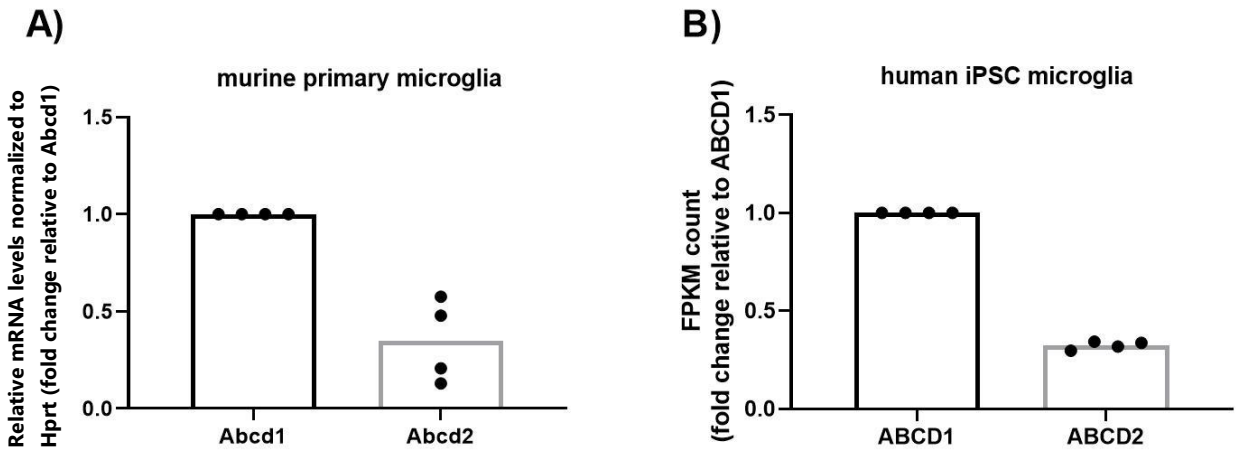

Figure 10 ***ABCD1/ABCD2 expression in human iPSC-derived microglia is comparable to Abcd1/Abcd2 expression in primary murine microglia.*** *(A) qRT-PCR analysis of Abcd1 and Abcd2 expression normalized to HPRT in microglia isolated from the brain of wild type mice (n=4). (B) Gene expression data for ABCD1 and ABCD2 in human iPSC-derived microglia, retrieved from the published RNA-seq data set GSE221013, (n=4) (Sabogal-Guáqueta u. a. 2023).*

mice at day 7 of in vitro culture with LPS (100 ng/ml) to a induce pro-inflammatory response or left cells untreated for 24 h before RNA was isolated and qRT-PCR was performed. As a general inflammatory mediator, we tested expression of the Tnfa gene encoding the pro-inflammatory cytokine TNFα which previously was found to be upregulated in LPS-treated X-ALD macrophages (Weinhofer u. a. 2018). As an anti-inflammatory marker, expression of the Abca1 gene was chosen, to investigate the cellular capacities of resolving inflammation. As shown in Fig. 11, our results from the qRT-PCR analysis revealed that as expected, both TNFα and Abca1 mRNA levels were upregulated by the 24 h LPS treatment. However, when we compared the expression levels between X-ALD and control microglial cells, no statistically significant difference could be observed (Fig. 11).

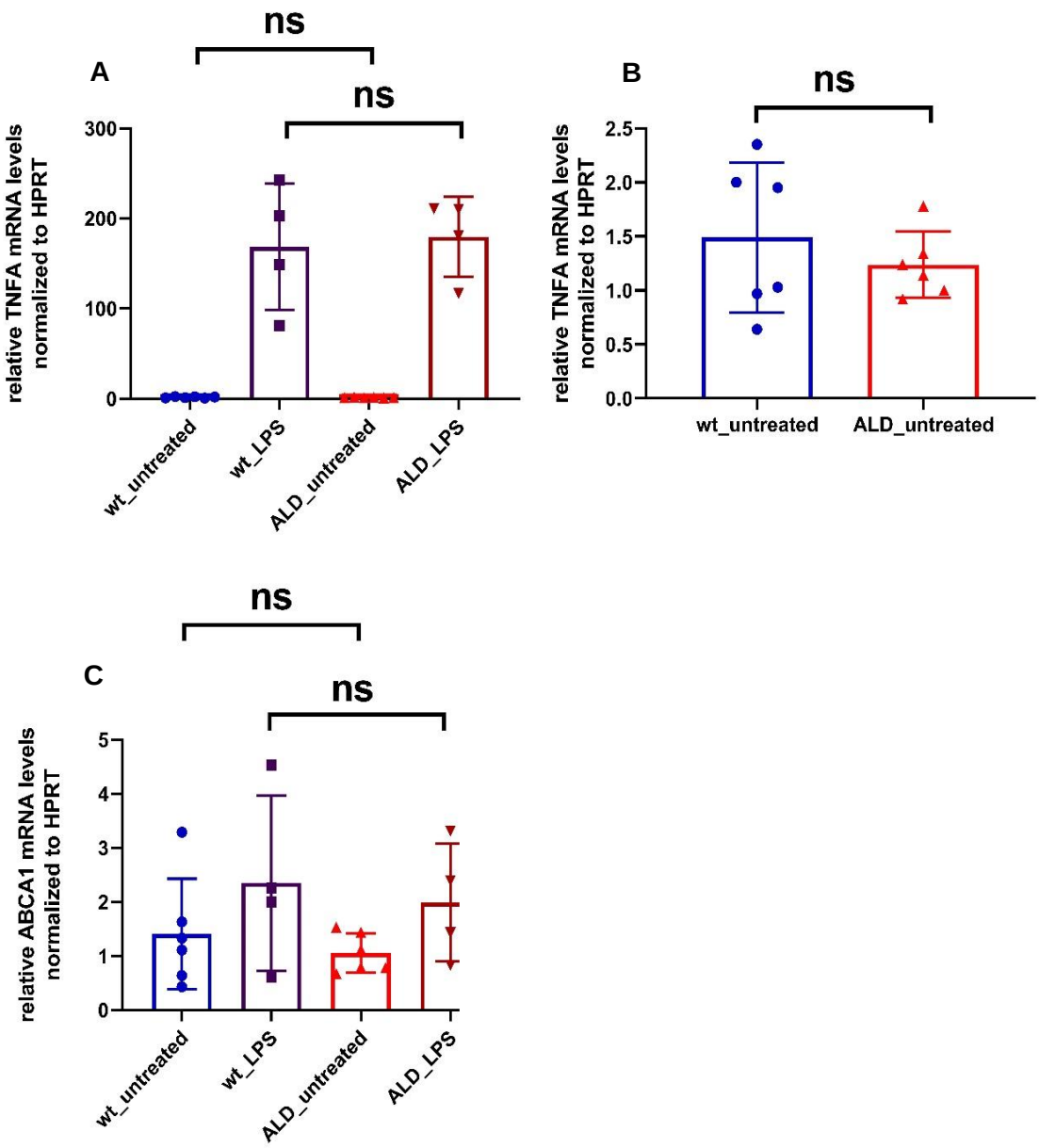

Figure 11 ***qRT-PCR analysis of X-ALD and wildtype murine microglial cells exposed to LPS.*** *X-ALD and wildtype microglial cells were cultivated for 7 days (X-ALD: n=6; wt: n=6) before being exposed to LPS (100 ng/ml) for 24 h (X-ALD: n=4; wt: n= 4) and (A,B) Tnfa and (B) Abca1 expression being assessed by qRT-PCR analysis. Wt and X-ALD microglial inflammatory response to LPS stimulation is the same. Statistical differences were calculated using two-tailed unpaired t-test. Data shown as mean ± standard deviation, n.s, non-significant, p>0.05.*

To address the phagocytic capacity of murine X-ALD microglial cells, we next used density gradient centrifugation to isolate myelin from the brains of X-ALD (n=9) and wt mice (n=9). Dissolved in 1x PBS, a total of 3.1 mL wild-type and 2.9 mL ALD myelin could be obtained in 3 isolations with protein concentrations of 55.9 mg/mL for wild-type myelin and 66.1 mg/mL for ALD myelin. To test the myelin enrichment in the isolated fraction, western blotting using an antibody directed against the myelin basic protein (Mbp), a protein highly enriched in myelin, was carried out (Fig. 12). To control for putative microglial and neuronal contamination, membranes were hybridized using antibodies against Iba-1 and synaptophysin, respectively (Fig. 12).

As shown in Fig. 12, an enrichment in myelin compared to whole brain homogenate (WBH) was observed in all 3 isolations carried out from brains of both wt (*Fig.* 12 A) and *Abcd1*-/y deficient X-ALD mice (*Fig.* 12 B). Whereas the microglia contamination as assessed by Iba-1 staining was found to be negligible, we observed that some neuronal contamination, as assessed by synaptophysin staining, was present in two out of three isolated myelin fractions. However, as the amount of contamination was like previously isolated myelin fractions that had successfully been used for phagocytosis experiments, we preceded with testing the endotoxin contamination of isolated myelin. We measured an endotoxin concentration of 94.8×10^{-3} EU/mL for wild-type and 117.6×10^{-3} EU/mL for ALD myelin, both below the threshold for macrophage activation by endotoxins = 0.27 EU/mL. For phagocytosis, the isolated myelin pools were labeled using the pH-sensitive pHrodo-green dye. A total of 3.1 mL wild-type and 2.9 mL ALD myelin could be obtained in 3 isolations. The protein concentration was determined to be 55.9 mg/mL for wild-type myelin and 66.1 mg/mL for ALD myelin.

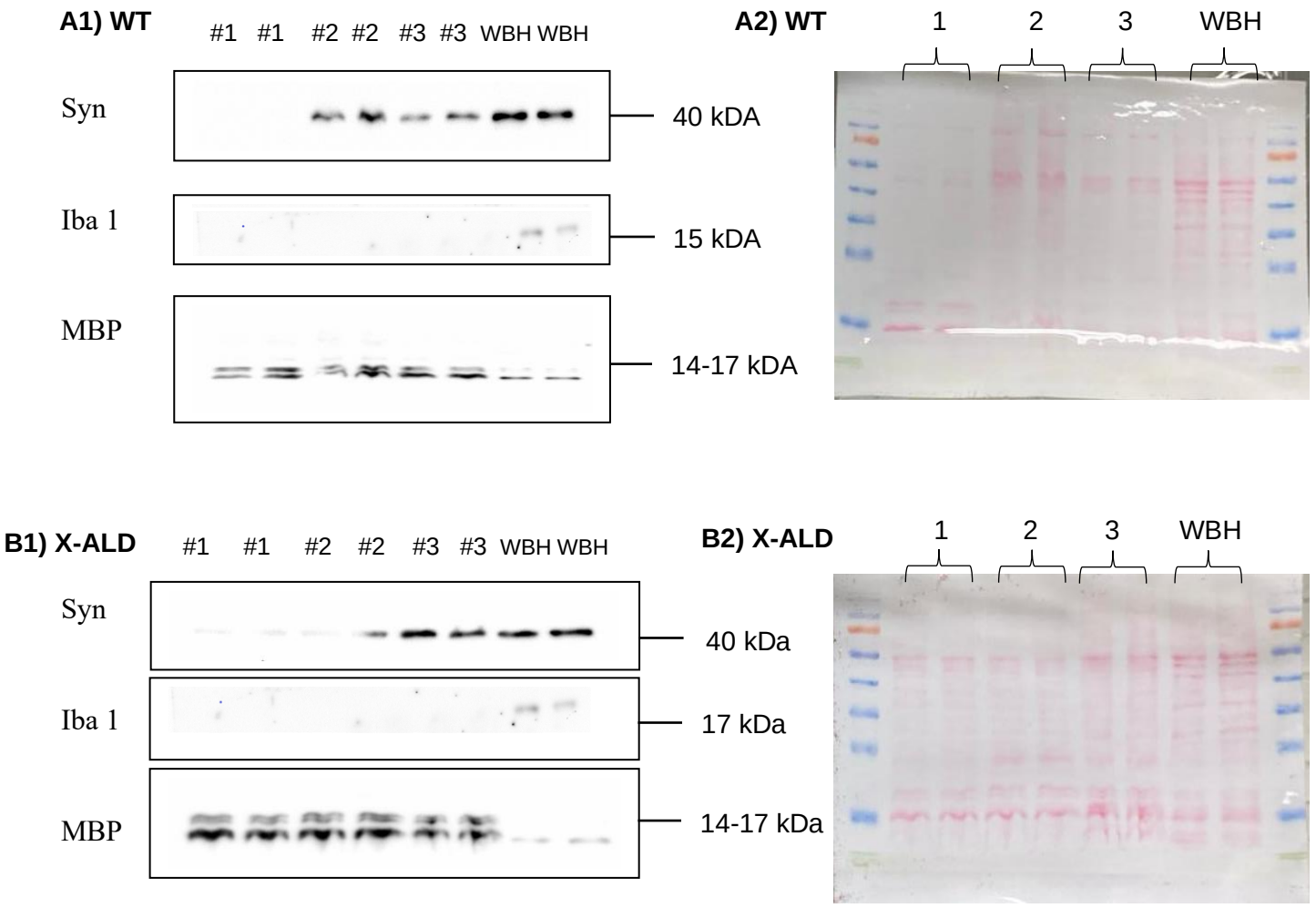

Figure 12 ***Western blot analysis of isolated myelin from X-ALD and control mice****. Western blot analysis of three myelin fractions isolated from either B) Abcd1-/y or A) wildtype mice and whole brain homogenate (WBH) as a control. The immunoblots derived from(A) wildtype and (B) X-ALD mice were probed with antibodies directed against Plp1, Iba-1 and synaptophysin to verify enrichment of myelin and the absence of contamination by microglia and neurones. As a control for loading, ponceau stains are shown.*

Abcd1-deficiency in primary murine microglia is associated with increased phagocytic uptake of ALD myelin

Using pHrodo-green labeled ALD myelin from X-ALD mice, we next assessed the phagocytic capacity of isolated microglial cells form X-ALD mice (n=3) and controls (n=3). After isolation and cultivation for 5 days in media supplemented with M-CSF, the microglial cells were exposed to 10 µg/ml pHrodo-green labeled ALD myelin before the phagocytic uptake was assessed by Incucyte live imaging for a duration of 48 h. For visualization of cells and automatic determination of cell number, the lipofuscin autofluorescence, emitted from microglia between 578-639 nm and detectable in the orange/red channel of the Inucyte, was used (Fig. 5A,B).

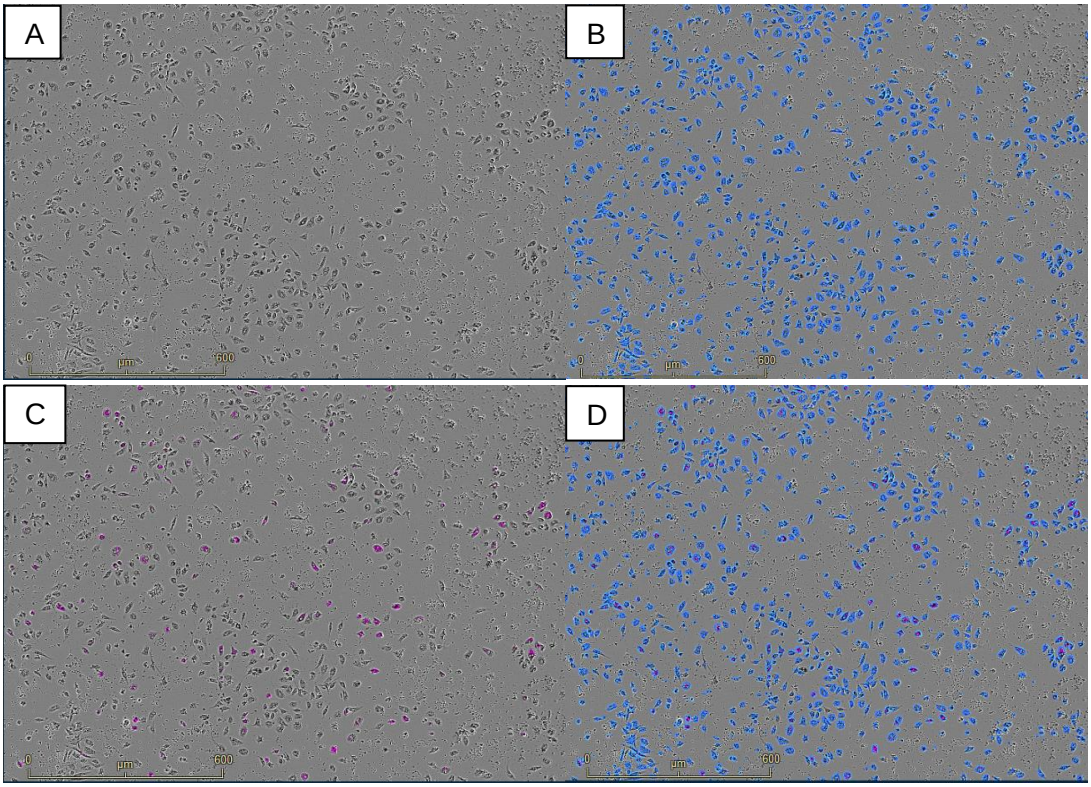

Figure 13 ***Abcd1-deficient primary murine microglia incubated with ALD myelin for 24 h.*** *Cells were imaged using the Incucyte 10x objective in the phase-contrast channel. Cell morphology visualized by (A) phase imaging and (B) autofluorescence of cells in the orange channel derived from liposuscin fluorescence, pseudocolored in blue. (C) Visualization of pHrodo-green labelled myelin uptake in the green channel with pseudocolor magenta assigned to the green fluorescence. (D) Overlay of autofluorescence and pHrodo-green signals to indicate microglial cells positive for myelin uptake.*

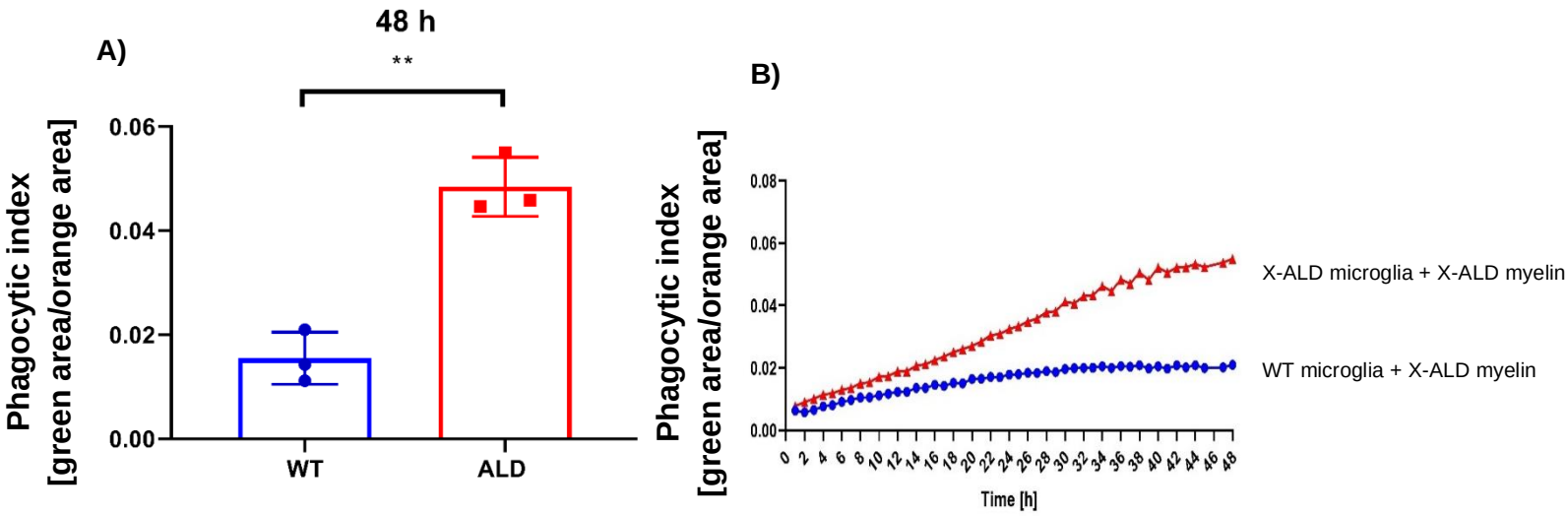

Figure 14 ***The phagocytic index of X-ALD primary murine microglia is significantly increased when compared to wild type cells***. *(A) For statistical analysis of the phagocytic indices of X-ALD and wild type primary murine microglia, the data observed at time point 48h was assessed. Statistical differences were calculated using a two-tailed unpaired t-test (n=3) Data shown as mean ± standard deviation, black asterisks indicate statistically significant differences. ** p ≤ 0.01. (B) Time course of the phagocytic index of a representative live imaging experiment involving X-ALD (red) and wild type (blue) primary murine microglia imaged in Incucyte live imaging for up to 48 h. Phagocytosis was normalized to cell count = phagocytic index. Timepoint 0 = 20 min after addition of X-ALD myelin. Pictures were taken every hour for 48h.*

When taken up by the microglial cells and entering the acidic lysosomal compartment, the green fluorescence emitted by the pHrodo-labelled ALD myelin (494-533 nm) could be detected in the green channel (Fig. 5C). Upon normalization of the phagocytosis rate to the number of microglial cells, the phagocytic capacity ("phagocytic index") could be determined. Together our phagocytic uptake experiments carried out with microglia isolated from 3 X-ALD and 3 control mice revealed that the phagocytosis of ALD myelin debris is significantly elevated in X-ALD mice when compared to healthy controls (Fig. 14).

Application of the CD36 inhibitor sulfosuccinimidyl oleate (SSO) normalizes the elevated phagocytic capacity in murine Abcd1-deficient microglial cells.

Sulfo-N-succinimidyl oleate (SSO) acts as a competitive inhibitor of the phagocytosis receptor CD36 (Kuda u. a. 2013), a main receptor involved in the uptake of myelin and previously found to be upregulated on mRNA level in X-ALD macrophages (Weinhofer et al., unpublished observation). To examine whether inhibition of CD36 through SSO application is able to normalize the elevated uptake of myelin in X-ALD microglial cells, cells were incubated with 10 µM SSO for 2h before the addition of pHrodo labeled X-ALD myelin and Incucyte live imaging being carried out for 48h.

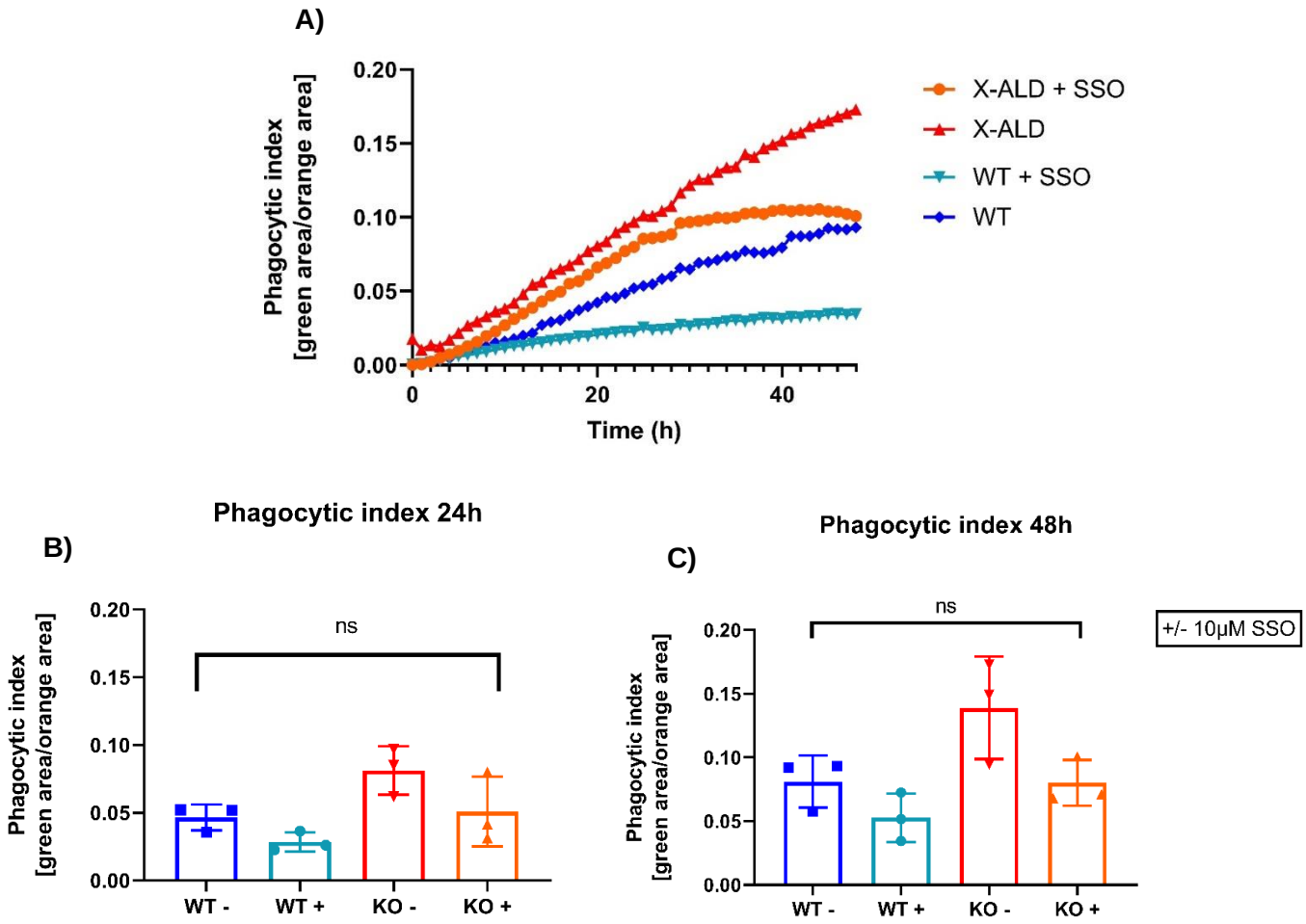

Figure 15 ***CD36 inhibition by SSO pre-treatment normalizes the elevated uptake of myelin in X-ALD primary murine microglial cells.*** *A) Representative time course of pHrodo labeled myelin uptake by wild type and X-ALD microglia. Cultured Abcd1-deficient and wt microglia were pre-treated with 10 µM SSO or DMSO solvent control for 2 h before pHrodo-green labeled ALD myelin was added and the phagocytic uptake was measured by Incucyte live imaging for 48h. Both X-ALD and wt microglia demonstrated decreased phagocytosis rates when exposed to 10 µM SSO Phagocytosis was normalized to cell count = phagocytic index. Timepoint 0 = 20 min after addition of X-ALD myelin. Pictures were taken every hour for 48h. B,C) Primary murine X-ALD and wt microglia with or without SSO (+/-): phagocytic index, normalized to cell number. Statistical differences were calculated using two-tailed unpaired t-test after 24h (B) and 48h (C) of phagocytosis (n=3) Data shown as mean ± standard deviation. Ns, non-significant (p>0.05).*

The addition of 10 µM SSO had no cytotoxic effect on either X-ALD or wt microglial cells, as indicated by similar morphology between treated and untreated cells. We found that the application of ALD myelin resulted in a higher uptake by Abcd1 deficient microglia when compared to wt cells, thus confirming our results presented in Fig. 6. When cells were pre-treated with 10 µM SSO for 2 h, we observed a lowering of phagocytosis with no adverse effects on the cells in X-ALD and wt microglia. Importantly, our data revealed that SSO pre-treatment normalized the elevated

uptake of ALD myelin in X-ALD cells to untreated wt levels when assessed at 24 and 48 h upon start of live imaging (Fig. 15).

Quantification of the normalized phagocytic index of both wt and X-ALD microglia at 24h (Fig. 15 B) or 48h (Fig. 15 C) upon application of pHrodo-labeled ALD myelin revealed that blocking the CD36 receptor by pre-treatment with SSO normalized the elevated phagocytic index of X-ALD cells to those observed for untreated wt cells.

SSO reduces the phagocytic uptake of myelin in X-ALD macrophages and healthy controls

So far, our data revealed that like human X-ALD macrophages, also primary microglial cells isolated from the brain of X-ALD mice present with increased phagocytic uptake of myelin debris. As we found that pre-treatment of X-ALD microglial cells with the CD36 inhibitor SSO normalized the elevated phagocytosis rate to wt levels, we next set out to test whether also in X-ALD macrophages the phagocytosis could be reduced by application of SSO.

We differentiated monocytes isolated from the blood of X-ALD patients and healthy controls for 7 days in the presence of M-CSF. Then cells were pre-treated with 100 µM SSO or DMSO solvent control for 2 h, before ALD myelin was added and the phagocytic uptake was measured by Incucyte live imaging for a total duration of 48 h. As expected, we observed increased uptake of ALD myelin by X-ALD macrophages, thus confirming previous observations (Fig. 19). The pre-treatment with SSO decreased the phagocytosis of ALD myelin in both X-ALD macrophages and healthy controls (Fig. 19) with a tendency toward stronger decrease in X-ALD cells, although not reaching statistically significance.

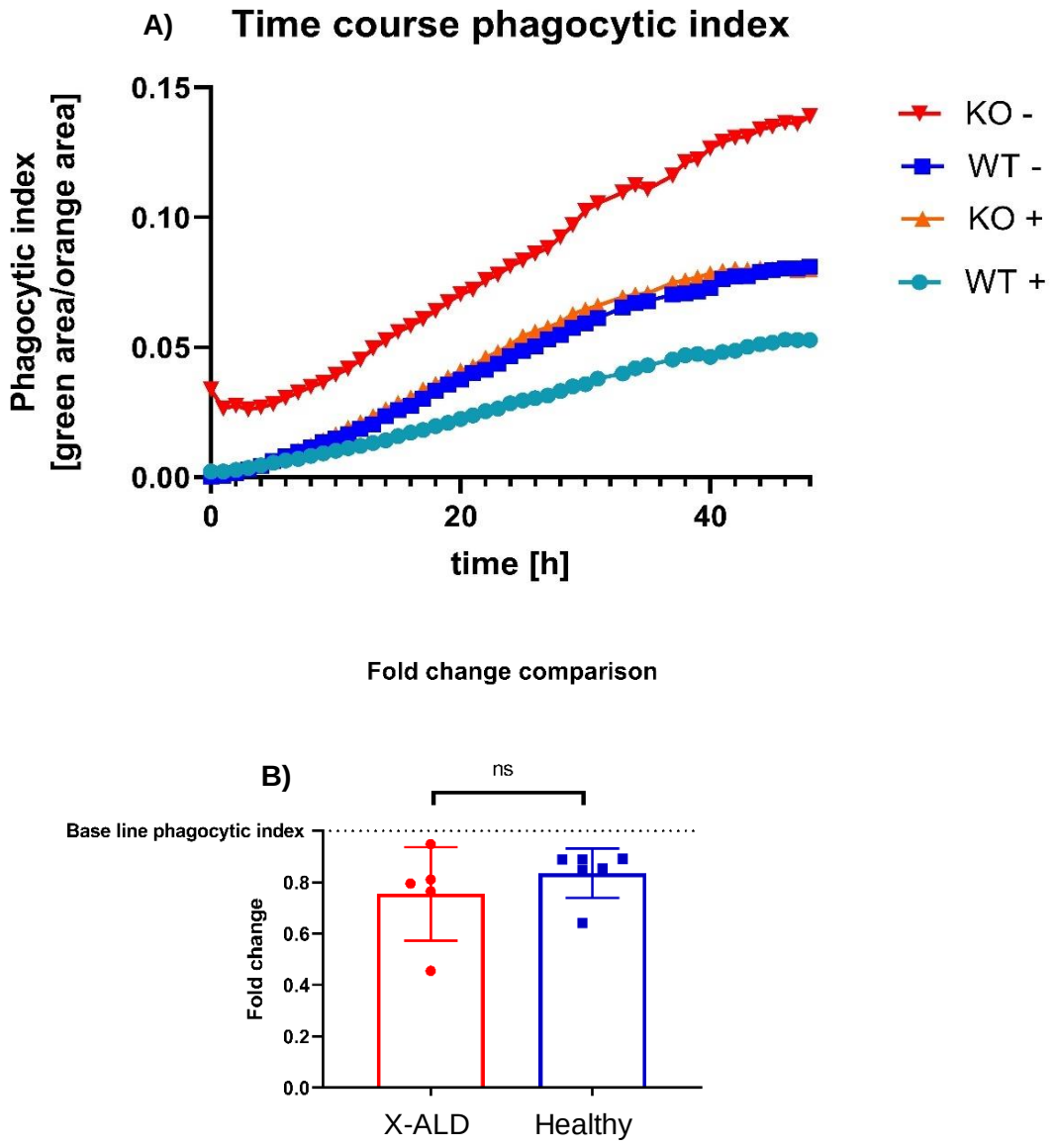

Figure 16 **CD36 inhibition by SSO pre-treatment reduces the elevated uptake of ALD myelin in human X-ALD macrophages.** Cultured Abcd1-deficient and healthy human macrophages were pre-treated with 100 µM SSO or DMSO solvent control for 2 h before pHrodo-green labeled ALD myelin was added and the time course of the phagocytic uptake was measured by Incucyte live imaging for 48h. (A) Time course of pHrodo labeled myelin uptake by wt and X-ALD microglia with SSO or DMSO. The graph represents the average of data derived from cells from 3 X-ALD patients and three healthy controls. Phagocytosis was normalized to cell count = phagocytic index. Timepoint 0 = 20 min after addition of X-ALD myelin. Pictures were taken every hour for 48h. (B) Comparison of fold-change decrease between healthy and X-ALD macrophages upon exposure to SSO. Statistical differences were calculated using two-tailed paired t-test after 24h (B) of phagocytosis (n= 5 X-ALD, n = 6 healthy control) Data shown as mean ± standard deviation. Ns, non-significant (p>0.05).

The scavenger receptor CD36 is highly expressed in mouse microglia but not further upregulated in X-ALD cells

Our results show that the elevated uptake of ALD myelin by macrophages and microglial cells could be normalized by application of the competitive CD36 inhibitor SSO. To further investigate the underlying mechanism and the role of CD36 in the increased phagocytic capacity of X-ALD cells, we next assessed the expression of CD36 in X-ALD cells. As shown in Fig. 17, our results from the qRT-PCR analysis revealed that as observed in macrophages, CD36 mRNA levels were upregulated by the 24 h LPS treatment. However, when we compared the expression levels between X-ALD and control microglial cells, no statistically significant difference could be observed in either LPS treated our untreated control cells (Fig. 11).

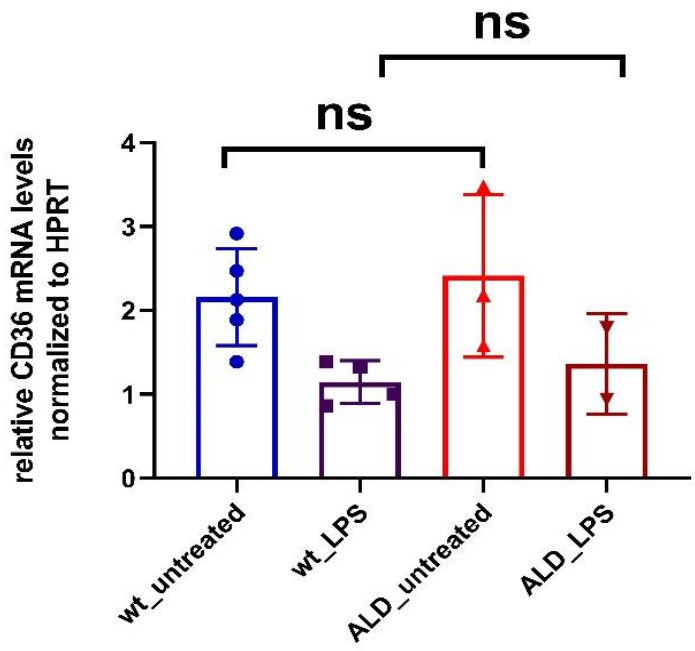

Figure 17 ***qRT-PCR analysis of X-ALD and wildtype murine microglial cells exposed to LPS.*** *X-ALD and wildtype microglial cells were cultivated for 7 days (X-ALD: n=6; wt: n=6) before being exposed to LPS (100 ng/ml) for 24 h (X-ALD: n=4; wt: n= 4).* Wt and X-ALD microglial inflammatory response to LPS stimulation in terms of downregulating CD36 expression is similar in X-ALD and wt cells. Statistical differences were calculated using two-tailed unpaired t-test. Data shown as mean ± standard deviation, p = 0.05. ns p ≥ 0.05.

CD36 and CD204 are not differentially expressed between ABCD1 deficient human macrophages and healthy control macrophages.

Our previous whole transcriptome analysis of macrophages derived from X-ALD patients and healthy controls revealed significant upregulation of genes involved in myelin uptake and phagocytosis such as CD36 and CD204. To elucidate whether the increased transcription of CD36 and CD204 is also reflected on protein level by increased presence of these receptors on the cell surface of macrophages, flow cytometry using fluorescently labelled antibodies targeting CD36 and CD204 was conducted. Importantly, thus far only receptors expressed on the cellular membrane were assessed, leaving to information about intracellular CD36/CD204 concentrations. Our data shown in Fig. 18 revealed that surface presence of neither CD36 nor CD204 was increased in X-ALD macrophages. In both genotypes, exposure of macrophages to ALD myelin throughout the 7-day differentiation process (23.3 µg/mL) lead to a similar significant decrease in CD36 expression, likely as a form of feedback mechanism in response to prolonged lipid phagocytosis.

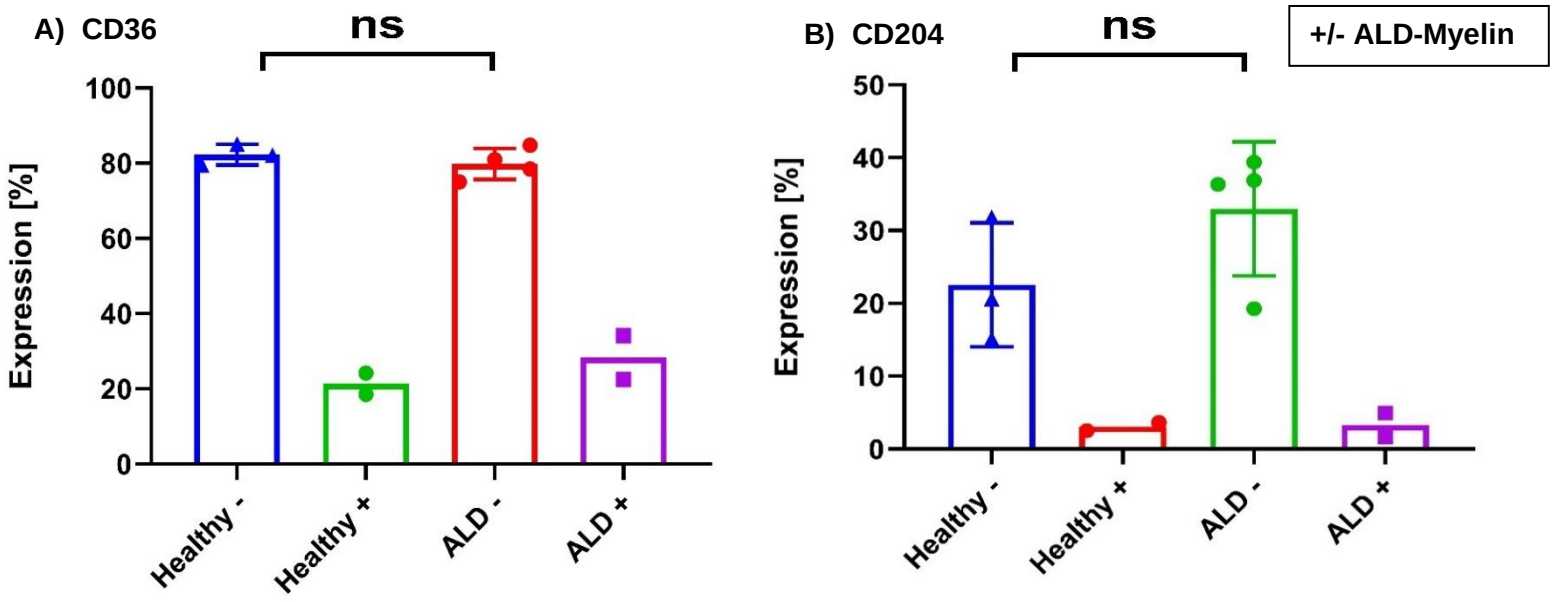

Figure 18 ***Flow cytometry to assess the surface expression of CD36 and CD204 in X-ALD and healthy control macrophages.*** *Monocytes from X-ALD patients or healthy controls were differentiated for 7d with or without ALD myelin before being harvested and stained for FACS. A) Indicates the number of CD36 positive cells in both X-ALD and control macrophages. B) Indicates the number of CD204 positive cells in both X-ALD and control macrophages. Statistical differences were calculated using paired t-test (n=3 healthy controls without myelin, n=2 healthy control with myelin, n=4 AMN without myelin, n=2 AMN with myelin). Data shown as mean ± standard deviation, p = 0.05, n.s. non significant.*

Discussion

Despite the monogenic defect of ABCD1 that underlies X-ALD, it presents as a clinically heterogeneous disease with no genotype-phenotype correlation. While the core form of X-ALD, AMN, is characterized by a slowly progressive, non-inflammatory axonopathy of the spinal cord long tracts, the severe life-threatening cerebral form, CALD, presents as a rapidly progressive brain inflammation, entailing demyelination and neurodegeneration (Engelen u. a. 2012). To date, the only therapeutic options for CALD involve HSCT and gene therapy, both only effective when applied in the early stages of the disease. The key to offer improved treatment strategies, possibly applicable also to more advanced disease stages, lies in the understanding of the mechanisms underlying X-ALD pathophysiology. ABCD1 deficiency leads to the accumulation of VLCFAs in tissues and body fluids of patients, with cells involved in lipid uptake and metabolism being especially affected. This places peripheral monocyte-derived macrophages and brain innate, yolk-sac derived microglial cells among the cell types metabolically most affected by ABCD1 deficiency, rendering these phagocytes interesting targets for investigation and potential intervention in the pathophysiology of X-ALD.

Neuroinflammation associated with brain white matter destruction is a hallmark of CALD, a process that involves microglia, the resident immune cells of the brain and CNS infiltrating macrophages (Turk u. a. 2020). It has recently been demonstrated that macrophages are pro-inflammatory skewed in X-ALD and lack the ability to adapt an anti-inflammatory phenotype that would be necessary to resolve the cause of the inflammation (Weinhofer u. a. 2018). For X-ALD microglia, so far no study addressed how the lack of ABCD1 would impair their functionality in terms of pro-inflammatory response or phagocytosis of myelin. With this work, we addressed this lack in knowledge by isolating microglial cells from the brain of X-ALD mice and characterizing their phagocytic function using Incucyte live imaging. In addition, we assessed whether the pro-inflammatory skewing in response to LPS treatment is not only present in human X-ALD macrophages but also in murine microglial cells.

With our study, we were able to replicate findings previously observed in human X-ALD macrophages in terms of increased phagocytosis of myelin debris. Using Incucyte live cell imaging conducted in 3 independent experiments and involving microglial cells isolated from 3 X-ALD and wt mice, we could demonstrate that the phagocytic uptake of pHrodo-green labelled ALD myelin is increased in Abcd1 deficient microglia when compared to wt microglia. The nearly 3-fold increase of the phagocytic index after 48h in X-ALD cells might point to a detrimental role of microglia under conditions of inflammatory demyelination in cerebral lesions. Of note, activated, pro-inflammatory microglia have been reported to mediate neurophagy (Vilalta und Brown 2018), the engulfment of live synapses next to myelin, possibly leading to the detrimental effects observed in CALD.

Interestingly, we observed that wt microglia and Abcd1 deficient microglia display different receptor kinetics: while in wt cells the phagocytic index reached a plateau after 24 h, Abcd1 deficient microglia showed no flattening of the curve with steady increase of the phagocytic index. It is tempting to speculate that X-ALD microglial cells possibly present with alterations in feed-back mechanisms that would normally prevent the overload of phagocytic cells with lipids, thus preventing the formation of foam cells. Possibly, a dysregulation of CD36 expression causes Abcd1 deficient microglia to stabilize or persistently transport CD36 to the cellular surface, thereby continuously increasing the phagocytic index, while wt cells can respond to prolonged phagocytosis by downregulating CD36 expression. However, despite being an attractive hypothesis, our results based on qPCR analysis do not support alterations in CD36 expression in X-ALD microglia. Alternatively, stabilization or upregulation of phagocytic receptors due to the accumulation of VLCFAs might possibly alter the uptake kinetics of X-ALD microglia. Importantly, upregulation of phagocytic receptors was previously observed using whole transcriptome RNA-sequencing of X-ALD macrophages (Weinhofer et al., unpublished observations). However, our FACS analysis revealed that there was no increased cell surface presence of the CD36 receptor in human X-ALD macrophages when compared to control cells. Thus, future studies should be addressed to investigate whether the upregulation of CD36 observed in our whole transcriptome RNA-sequencing study on X-ALD macrophages might be reflected by increased intracellular pools of CD36, that might further contribute to increases CD36 cell membrane density in response to myelin turnover. An alternative explanation for the diverging

results between CD36 RNA and protein levels in human X-ALD macrophages could be that the human X-ALD monocyte-derived macrophages used in the FACS studies were derived from monocytes that were isolated from the blood of patients using a slightly different isolation protocols. In this method, non-classical and intermediate monocytes were removed from the monocyte pool using antibodies directed against $CD16^{+}$, leaving classical monocytes only in the isolated fraction. However, next to classical monocytes also intermediate monocytes present with a high level of CD36 (Kapellos u. a. 2019), which might contribute to the lack of increased CD36 surface receptor expression in X-ALD macrophages when compared to healthy macrophages. Likewise, no increased CD204 expression was found in either microglia or macrophages. Again, the intracellular pool of CD204 was not assessed but might also influence myelin uptake in either microglia or macrophages. In the case of microglia, the isolation process itself might also have influenced CD204 expression and altered the results.

So far, our studies are limited to primary murine microglial cells lacking Abcd1. However, future experiments will be addressed to investigate whether also in human microglial cells the deficiency of ABCD1 is immanently associated with upregulation of phagocytosis. For this approach, human iPSC-derived microglial cells will be used that will be gene edited for ABCD1 using CRISPR/Cas9 technology. To this end, we compared expression of ABCD1 and the related ABCD2 gene in our data derived from qPCR analysis and a publicly available RNA-sequencing dataset generated from human iPSC-derived microglial cells (Sabogal-Guáqueta u. a. 2023, GSE221013). ABCD1/ABCD2 expression pattern has been described as „mirror-like“, with distinct expression patterns especially in the brain but overlapping function, with ABCD2 being able to functionally replace ABCD1 (Troffer-Charlier u. a. 1998). Our analysis revealed that the ratio of expression between ABCD1 and ABCD2 is similar within the two species, supporting attempts to investigate the lack of ABCD1 function also in murine X-ALD microglial cells.

Interestingly, when we compared in detail the uptake kinetics of murine microglial cells and human macrophages, we observed that murine microglial cells presented with a linear phagocytic response to myelin, whereas human monocyte-derived macrophages displayed sigmoidal curves. This might probably hint to different regulatory mechanism underlying phagocytosis in either cell type. In this context, it is relevant to consider that microglia have been reported to display higher

capacities to phagocytose myelin than macrophages (Andoh und Koyama 2021), possibly causing the differences in receptor kinetics. Perhaps the flattening of the curve would be observed in microglial phagocytosis as well when the imaging would be continued above 48h.

The upregulation of phagocytosis seems to be immanent to X-ALD microglia and macrophages, closely linking the lack of ABCD1 and concomitant accumulation of VLCFAs to this process. Accordingly, we set out to investigate how the altered phagocytic ability in X-ALD phagocytes could be rescued by pharmacological treatment. In 3 independent experiments, involving microglial cells isolated from the brains of 3 wt and 3 Abcd1 deficient murine microglia, we demonstrated that pre-treatment with the pharmacological compound SSO was able to reduce the increased phagocytic index of Abcd1 deficient microglia to wt levels. SSO is a sterically demanding oleic acid derivative that binds the CD36 fatty acid translocase and myelin uptake receptor in a competitive manner, thereby reducing CD36 mediated uptake of myelin in both wt and X-ALD murine microglia. Concentrations as low as 10 µM were found to suffice to achieve reduction of the phagocytic index of Abcd1 deficient murine microglia to the levels of phagocytic index displayed by wt murine microglia, with no observed adverse effects on viability. In terms of receptor kinetics, murine X-ALD microglia exposed to SSO demonstrated a drastic flattening of the curve after around 24h, whereas wt cells exposed to the applied concentration of SSO showed only a marginal phagocytic index with a very shallow slope. Accordingly, these results may indicate that pre-treatment with SSO leads to modulation of the receptor kinetics in X-ALD cells, akin to the wt response to myelin.

Importantly, we were able to replicate the reduction of phagocytic indices upon exposure to SSO also in human monocyte-derived macrophages. Using macrophages derived from 5 X-ALD patients and 6 healthy controls and pre-treatment with 100 µM SSO, we were able to reduce the phagocytic index associated with the lack of ABCD1 also in the human context. Of note, opposite to murine microglia, 10 µM SSO were found to be ineffective in significantly reducing the phagocytic capability of macrophages (data not shown), indicating differences in the response of microglia and macrophages towards the CD36 inhibitor. Whereas the response between human X-ALD macrophages and healthy control cells with regard to reduction of the myelin uptake upon SSO pre-treatment did not differ significantly between the genotypes, a slight tendency towards

stronger reduction in X-ALD cells was observed. Also in human macrophages, no adverse effects of SSO pre-treatment on viability of cells were observed. Together, these findings demonstrate the involvement of the CD36 fatty acid translocase in myelin phagocytosis in both murine microglia and human macrophages. Future studies should be addressed to investigate, whether pharmacologically targeting CD36-mediated uptake of VLCFAs or VLCFA-enriched myelin debris might be beneficial also in the context of CALD patients.

Next to the phagocytic capability of microglial cells, we also investigated their inflammatory response in the absence of Abcd1. Using microglial cells isolated from the brain of 6 wt and X-ALD mice and cultivated for 7 days, we analyzed the upregulation of the pro-inflammatory mediator Tnfa upon exposure of cells to LPS for 24h. We found that in both LPS challenged and control primary murine microglia, X-ALD and wt cells showed the same expression levels of Tnfa, indicating a similar response to inflammatory stimuli in both genotypes. In addition to Tnfa expression, Abca1 mRNA levels were assessed in response to LPS stimulation. The Abca1 encodes an ABC-transporter located at the plasma membrane whose gene expression is upregulated in response to the anti-inflammatory transcription factor LXRα (Yin, Liao, und Tang 2010). Thus, increased Abca1 expression indicates initiation of the anti-inflammatory response that enables termination of the acute pro-inflammatory phase. However, as with Tnfa, we found no dysregulation in X-ALD microglia when compared to wt cells in LPS challenged or unchallenged conditions.

It must be noted that especially the FACS results derived from human X-ALD macrophages might require additional experimental verification involving monocyte populations isolated by similar isolation protocols. Despite the similar ABCD1/Abcd1 and ABCD2/Abcd2 expression ratios in primary murine microglia and human iPSC microglia, species differences might still likely affect their phagocytic and inflammatory responses. Those differences become especially apparent when considering the lack of CALD phenotype in mice and the late and only mild development of AMN-like symptoms in X-ALD mice (Biffi, Aubourg, und Cartier 2011).
Accordingly, future experiments will be conducted using human iPSC microglia gene edited for ABCD1 that will involve a detailed investigation of intracellular receptors and additional phagocytic substrates beside X-ALD myelin. Confocal fluorescence imaging will be conducted to

elucidate intracellular trafficking pathways of phagocytic cargo in hopes of finding the cause on increased phagocytic indices. Finally, the response to pro-inflammatory stimuli in addition to LPS, belonging to the group of altered-self inflammatory stimuli, will be assessed in a timely manner.

In summary we have shown that next to human macrophages also X-ALD and wt primary murine microglia display differences in the uptake of X-ALD myelin with Abcd1 deficient cells showing an increased phagocytic index when compared to wt cells. Further we could demonstrate that administration of the competitive CD36 inhibitor SSO in differing concentrations is able to reduce the increased phagocytic indices of both human monocyte-derived macrophages and primary murine microglia back to the levels of their respective wt/healthy control counterparts. Despite not being able to trace those differences back to altered inflammatory response in either cell type yet, those results potentially hold the key to novel therapeutic strategies in X-ALD.

Bibliography

Abel, Soeren, Christian Hundhausen, Rolf Mentlein, Alexander Schulte, Theo A. Berkhout, Neil Broadway, Dieter Hartmann, u. a. 2004. „The Transmembrane CXC-Chemokine Ligand 16 Is Induced by IFN-γ and TNF-α and Shed by the Activity of the Disintegrin-Like Metalloproteinase ADAM10“. *The Journal of Immunology* 172 (10): 6362–72. https://doi.org/10.4049/jimmunol.172.10.6362.

Andoh, Megumi, und Ryuta Koyama. 2021. „Comparative Review of Microglia and Monocytes in CNS Phagocytosis“. *Cells* 10 (10): 2555. https://doi.org/10.3390/cells10102555.

Asheuer, Muriel, Françoise Pflumio, Sonia Benhamida, Anne Dubart-Kupperschmitt, Françoise Fouquet, Yoshinori Imai, Patrick Aubourg, und Nathalie Cartier. 2004. „Human CD34 $^{+}$ Cells Differentiate into Microglia and Express Recombinant Therapeutic Protein“. *Proceedings of the National Academy of Sciences* 101 (10): 3557–62. https://doi.org/10.1073/pnas.0306431101.

Berger, Johannes, Aurora Pujol, Patrick Aubourg, und Sonja Forss-Petter. 2010. „Current and Future Pharmacological Treatment Strategies in X-Linked Adrenoleukodystrophy“. *Brain Pathology* 20 (4): 845–56. https://doi.org/10.1111/j.1750-3639.2010.00393.x.

Bergner, Caroline G., Franziska Van Der Meer, Anne Winkler, Claudia Wrzos, Mevlude Türkmen, Emil Valizada, Dirk Fitzner, u. a. 2019. „Microglia Damage Precedes Major Myelin Breakdown in X-linked Adrenoleukodystrophy and Metachromatic Leukodystrophy“. *Glia* 67 (6): 1196–1209. https://doi.org/10.1002/glia.23598.

Biffi, A., P. Aubourg, und N. Cartier. 2011. „Gene Therapy for Leukodystrophies“. *Human Molecular Genetics* 20 (R1): R42–53. https://doi.org/10.1093/hmg/ddr142.

Botelho, Roberto J., und Sergio Grinstein. 2011. „Phagocytosis“. *Current Biology* 21 (14): R533–38. https://doi.org/10.1016/j.cub.2011.05.053.

Brown, Eric J. 1995. „Phagocytosis“. *BioEssays* 17 (2): 109–17. https://doi.org/10.1002/bies.950170206.

Bujold, Kim, David Rhainds, Christian Jossart, Maria Febbraio, Sylvie Marleau, und Huy Ong. 2009. „CD36-Mediated Cholesterol Efflux Is Associated with PPARγ Activation via a MAPK-Dependent COX-2 Pathway in Macrophages“. *Cardiovascular Research* 83 (3): 457–64. https://doi.org/10.1093/cvr/cvp118.

Chiesa, Robert, Jaap Jan Boelens, Christine N. Duncan, Jörn-Sven Kühl, Caroline Sevin, Neena Kapoor, Vinod K. Prasad, u. a. 2022. „Variables Affecting Outcomes after Allogeneic Hematopoietic Stem Cell Transplant for Cerebral Adrenoleukodystrophy“. *Blood Advances* 6 (5): 1512–24. https://doi.org/10.1182/bloodadvances.2021005294.

Dhungana, Hiramani, Mikko T. Huuskonen, Merja Jaronen, Sighild Lemarchant, Humair Ali, Velta Keksa-Goldsteine, Gundars Goldsteins, Katja M. Kanninen, Jari Koistinaho, und Tarja Malm. 2017. „Sulfosuccinimidyl Oleate Sodium Is Neuroprotective and Alleviates Stroke-Induced Neuroinflammation“. *Journal of Neuroinflammation* 14 (1): 237. https://doi.org/10.1186/s12974-017-1010-7.

Drover, Victor A., David V. Nguyen, Claire C. Bastie, Yolanda F. Darlington, Nada A. Abumrad, Jeffrey E. Pessin, Erwin London, Daisy Sahoo, und Michael C. Phillips. 2008. „CD36 Mediates Both Cellular Uptake of Very Long Chain Fatty Acids and Their Intestinal Absorption in Mice“. *Journal of Biological Chemistry* 283 (19): 13108–15. https://doi.org/10.1074/jbc.M708086200.

Eichler, Florian S., Jia-Qian Ren, Michael Cossoy, Anna M. Rietsch, Sameer Nagpal, Ann B. Moser, Matthew P. Frosch, und Richard M. Ransohoff. 2008. „Is Microglial Apoptosis an

Early Pathogenic Change in Cerebral X-linked Adrenoleukodystrophy?“ *Annals of Neurology* 63 (6): 729–42. https://doi.org/10.1002/ana.21391.
Elhelu, M. A. 1983. „The Role of Macrophages in Immunology“. *Journal of the National Medical Association* 75 (3): 314–17.
Engelen, Marc, Stephan Kemp, Marianne De Visser, Björn M Van Geel, Ronald Ja Wanders, Patrick Aubourg, und Bwee Poll-The. 2012. „X-Linked Adrenoleukodystrophy (X-ALD): Clinical Presentation and Guidelines for Diagnosis, Follow-up and Management“. *Orphanet Journal of Rare Diseases* 7 (1): 51. https://doi.org/10.1186/1750-1172-7-51.
Engelen, Marc, Stephan Kemp, und Bwee-Tien Poll-The. 2014. „X-Linked Adrenoleukodystrophy: Pathogenesis and Treatment“. *Current Neurology and Neuroscience Reports* 14 (10): 486. https://doi.org/10.1007/s11910-014-0486-0.
Feng, Yanan, Wenxiu Sun, Fengcui Sun, Guoliang Yin, Pengpeng Liang, Suwen Chen, Xiangyi Liu, Tongfei Jiang, und Fengxia Zhang. 2022. „Biological Mechanisms and Related Natural Inhibitors of CD36 in Nonalcoholic Fatty Liver“. *Drug Design, Development and Therapy* Volume 16 (November):3829–45. https://doi.org/10.2147/DDDT.S386982.
Garden, Gwenn A., und Thomas Möller. 2006. „Microglia Biology in Health and Disease“. *Journal of Neuroimmune Pharmacology* 1 (2): 127–37. https://doi.org/10.1007/s11481-006-9015-5.
Gong, Yi, Nikhil Sasidharan, Fiza Laheji, Matthew Frosch, Patricia Musolino, Rudy Tanzi, Doo Yeon Kim, Alessandra Biffi, Joseph El Khoury, und Florian Eichler. 2017. „Microglial Dysfunction as a Key Pathological Change in Adrenomyeloneuropathy“. *Annals of Neurology* 82 (5): 813–27. https://doi.org/10.1002/ana.25085.
Gordon, Siamon. 2016. „Phagocytosis: An Immunobiologic Process“. *Immunity* 44 (3): 463–75. https://doi.org/10.1016/j.immuni.2016.02.026.
Gordon, Siamon, und Luisa Martinez-Pomares. 2017. „Physiological Roles of Macrophages“. *Pflügers Archiv - European Journal of Physiology* 469 (3–4): 365–74. https://doi.org/10.1007/s00424-017-1945-7.
Grajchen, Elien, Elien Wouters, Britt Van De Haterd, Mansour Haidar, Kévin Hardonnière, Tess Dierckx, Jana Van Broeckhoven, u. a. 2020. „CD36-Mediated Uptake of Myelin Debris by Macrophages and Microglia Reduces Neuroinflammation“. *Journal of Neuroinflammation* 17 (1): 224. https://doi.org/10.1186/s12974-020-01899-x.
Haney, Michael S., Christopher J. Bohlen, David W. Morgens, James A. Ousey, Amira A. Barkal, C. Kimberly Tsui, Braeden K. Ego, u. a. 2018. „Identification of Phagocytosis Regulators Using Magnetic Genome-Wide CRISPR Screens“. *Nature Genetics* 50 (12): 1716–27. https://doi.org/10.1038/s41588-018-0254-1.
Höftberger, Romana, und Hans Lassmann. 2018. „Inflammatory Demyelinating Diseases of the Central Nervous System“. In *Handbook of Clinical Neurology*, 145:263–83. Elsevier. https://doi.org/10.1016/B978-0-12-802395-2.00019-5.
Husemann, Jens, John D. Loike, Roman Anankov, Maria Febbraio, und Samuel C. Silverstein. 2002. „Scavenger Receptors in Neurobiology and Neuropathology: Their Role on Microglia and Other Cells of the Nervous System“. *Glia* 40 (2): 195–205. https://doi.org/10.1002/glia.10148.
Jaspers, Yorrick R. J., Sacha Ferdinandusse, Inge M. E. Dijkstra, Rinse Willem Barendsen, Henk Van Lenthe, Wim Kulik, Marc Engelen, Susan M. I. Goorden, Frédéric M. Vaz, und Stephan Kemp. 2020. „Comparison of the Diagnostic Performance of C26:0-Lysophosphatidylcholine and Very Long-Chain Fatty Acids Analysis for Peroxisomal Disorders“. *Frontiers in Cell and Developmental Biology* 8 (Juli):690. https://doi.org/10.3389/fcell.2020.00690.
Jurga, Agnieszka M., Martyna Paleczna, und Katarzyna Z. Kuter. 2020. „Overview of General and Discriminating Markers of Differential Microglia Phenotypes“. *Frontiers in Cellular Neuroscience* 14 (August):198. https://doi.org/10.3389/fncel.2020.00198.

Kapellos, Theodore S., Lorenzo Bonaguro, Ioanna Gemünd, Nico Reusch, Adem Saglam, Emily R. Hinkley, und Joachim L. Schultze. 2019. „Human Monocyte Subsets and Phenotypes in Major Chronic Inflammatory Diseases“. *Frontiers in Immunology* 10 (August):2035. https://doi.org/10.3389/fimmu.2019.02035.

Kawaguchi, Kosuke, und Masashi Morita. 2016. „ABC Transporter Subfamily D: Distinct Differences in Behavior between ABCD1–3 and ABCD4 in Subcellular Localization, Function, and Human Disease“. *BioMed Research International* 2016:1–11. https://doi.org/10.1155/2016/6786245.

Kazakova, Elena, Pavel Iamshchikov, Irina Larionova, und Julia Kzhyshkowska. 2023. „Macrophage scavenger receptors: Tumor support and tumor inhibition“. *Frontiers in Oncology* 12 (Januar):1096897. https://doi.org/10.3389/fonc.2022.1096897.

Kelley, Jim L., Tammy R. Ozment, Chuanfu Li, John B. Schweitzer, und David L. Williams. 2014. „Scavenger Receptor-A (CD204): A Two-Edged Sword in Health and Disease“. *Critical Reviews in Immunology* 34 (3): 241–61. https://doi.org/10.1615/CritRevImmunol.2014010267.

Kemp, S., A. Pujol, H. R. Waterham, B. M. van Geel, C. D. Boehm, G. V. Raymond, G. R. Cutting, R. J. Wanders, und H. W. Moser. 2001. „ABCD1 Mutations and the X-Linked Adrenoleukodystrophy Mutation Database: Role in Diagnosis and Clinical Correlations“. *Human Mutation* 18 (6): 499–515. https://doi.org/10.1002/humu.1227.

Kemp, Stephan, Irene C. Huffnagel, Gabor E. Linthorst, Ronald J. Wanders, und Marc Engelen. 2016. „Adrenoleukodystrophy - Neuroendocrine Pathogenesis and Redefinition of Natural History“. *Nature Reviews. Endocrinology* 12 (10): 606–15. https://doi.org/10.1038/nrendo.2016.90.

Kemp, Stephan, und Ronald Wanders. 2010. „Biochemical Aspects of X-Linked Adrenoleukodystrophy“. *Brain Pathology* 20 (4): 831–37. https://doi.org/10.1111/j.1750-3639.2010.00391.x.

Kim, Seung U., und Jean De Vellis. 2005. „Microglia in Health and Disease“. *Journal of Neuroscience Research* 81 (3): 302–13. https://doi.org/10.1002/jnr.20562.

Korenke, G. Christoph, Ekkehard Wilichowski, Donald H. Hunneman, Folker Hanefeld, Sigrid Fuchs, Ernst Krasemann, und Helmuth G. Doerr. 1996. „Cerebral Adrenoleukodystrophy (ALD) in Only One of Monozygotic Twins with an Identical ALD Genotype“. *Annals of Neurology* 40 (2): 254–57. https://doi.org/10.1002/ana.410400221.

Kuda, Ondrej, Terri A. Pietka, Zuzana Demianova, Eva Kudova, Josef Cvacka, Jan Kopecky, und Nada A. Abumrad. 2013. „Sulfo-N-Succinimidyl Oleate (SSO) Inhibits Fatty Acid Uptake and Signaling for Intracellular Calcium via Binding CD36 Lysine 164: SSO Also Inhibits Oxidized Low Density Lipoprotein Uptake by Macrophages“. *The Journal of Biological Chemistry* 288 (22): 15547–55. https://doi.org/10.1074/jbc.M113.473298.

Kumar, Vijay. 2020. „Macrophages: The Potent Immunoregulatory Innate Immune Cells“. In *Macrophage Activation - Biology and Disease*, herausgegeben von Khalid Hussain Bhat. IntechOpen. https://doi.org/10.5772/intechopen.88013.

Lee, Sena J., Stefan Evers, Daniel Roeder, Albert F. Parlow, Juha Risteli, Leila Risteli, Y. C. Lee, Ten Feizi, Hanno Langen, und Michel C. Nussenzweig. 2002. „Mannose Receptor-Mediated Regulation of Serum Glycoprotein Homeostasis“. *Science (New York, N.Y.)* 295 (5561): 1898–1901. https://doi.org/10.1126/science.1069540.

Lloyd, Amy F., und Veronique E. Miron. 2019. „The Pro-Remyelination Properties of Microglia in the Central Nervous System“. *Nature Reviews Neurology* 15 (8): 447–58. https://doi.org/10.1038/s41582-019-0184-2.

Mallack, Eric J., Bela Turk, Helena Yan, und Florian S. Eichler. 2019. „The Landscape of Hematopoietic Stem Cell Transplant and Gene Therapy for X-Linked Adrenoleukodystrophy“. *Current Treatment Options in Neurology* 21 (12): 61. https://doi.org/10.1007/s11940-019-0605-y.

Nieman, Lynnette K., und Maria L. Chanco Turner. 2006. „Addison's Disease". *Clinics in Dermatology* 24 (4): 276–80. https://doi.org/10.1016/j.clindermatol.2006.04.006.
Nowak, Johannes, Ulrike Löbel, Matthias Wölfl, Paul-Gerhardt Schlegel, und Monika Warmuth-Metz. 2015. „MRI Demyelination Pattern and Clinical Course in a Child with Cerebral X-Linked Adrenoleukodystrophy (X-ALD)". *Acta Radiologica Open* 4 (4): 204798161557365. https://doi.org/10.1177/2047981615573655.
Ohue, Yoshihiro, und Hiroyoshi Nishikawa. 2019. „Regulatory T (Treg) Cells in Cancer: Can Treg Cells Be a New Therapeutic Target?" *Cancer Science* 110 (7): 2080–89. https://doi.org/10.1111/cas.14069.
Pathak, Divya, Neelay Mehendale, Shubham Singh, Roop Mallik, und Siddhesh S. Kamat. 2018. „Lipidomics Suggests a New Role for Ceramide Synthase in Phagocytosis". *ACS Chemical Biology* 13 (8): 2280–87. https://doi.org/10.1021/acschembio.8b00438.
Pujol, Aurora, Isidre Ferrer, Carme Camps, Elisabeth Metzger, Colette Hindelang, Noëlle Callizot, Montse Ruiz, Teresa Pàmpols, Marisa Giròs, und Jean Louis Mandel. 2004. „Functional Overlap between ABCD1 (ALD) and ABCD2 (ALDR) Transporters: A Therapeutic Target for X-Adrenoleukodystrophy". *Human Molecular Genetics* 13 (23): 2997–3006. https://doi.org/10.1093/hmg/ddh323.
Sabogal-Guáqueta, Angélica María, Alejandro Marmolejo-Garza, Marina Trombetta-Lima, Asmaa Oun, Jasmijn Hunneman, Tingting Chen, Jari Koistinaho, u. a. 2023. „Species-Specific Metabolic Reprogramming in Human and Mouse Microglia during Inflammatory Pathway Induction". *Nature Communications* 14 (1): 6454. https://doi.org/10.1038/s41467-023-42096-7.
Saharan, Ojal, Neelay Mehendale, und Siddhesh S. Kamat. 2022. „Phagocytosis: A (Sphingo)Lipid Story". *Current Research in Chemical Biology* 2:100030. https://doi.org/10.1016/j.crchbi.2022.100030.
Sailor, Kurt A., George Agoranos, Sergio López-Manzaneda, Satoru Tada, Beatrix Gillet-Legrand, Corentin Guerinot, Jean-Baptiste Masson, u. a. 2022. „Hematopoietic Stem Cell Transplantation Chemotherapy Causes Microglia Senescence and Peripheral Macrophage Engraftment in the Brain". *Nature Medicine* 28 (3): 517–27. https://doi.org/10.1038/s41591-022-01691-9.
Shah, Sahil, Lilly M. Wong, Kendra Ellis, Brittany Bodnar, Sami Saribas, Julia Ting, Zhengyu Wei, u. a. 2022. „Microglia-Specific Promoter Activities of HEXB Gene". *Frontiers in Cellular Neuroscience* 16 (März):808598. https://doi.org/10.3389/fncel.2022.808598.
Sierra, Amanda, Rosa C. Paolicelli, und Helmut Kettenmann. 2019. „Cien Años de Microglía: Milestones in a Century of Microglial Research". *Trends in Neurosciences* 42 (11): 778–92. https://doi.org/10.1016/j.tins.2019.09.004.
Soulet, Denis, und Serge Rivest. 2008. „Microglia". *Current Biology* 18 (12): R506–8. https://doi.org/10.1016/j.cub.2008.04.047.
Thomas, Graham D., Anouk A. J. Hamers, Catherine Nakao, Paola Marcovecchio, Angela M. Taylor, Chantel McSkimming, Anh Tram Nguyen, Coleen A. McNamara, und Catherine C. Hedrick. 2017. „Human Blood Monocyte Subsets: A New Gating Strategy Defined Using Cell Surface Markers Identified by Mass Cytometry". *Arteriosclerosis, Thrombosis, and Vascular Biology* 37 (8): 1548–58. https://doi.org/10.1161/ATVBAHA.117.309145.
Troffer-Charlier, Nathalie, Nathalie Doerflinger, Elisabeth Metzger, Françoise Fouquet, Jean-Louis Mandel, und Patrick Aubourg. 1998. „Mirror Expression of Adrenoleukodystrophy and Adrenoleukodystrophy Related Genes in Mouse Tissues and Human Cell Lines". *European Journal of Cell Biology* 75 (3): 254–64. https://doi.org/10.1016/S0171-9335(98)80121-0.
Turk, Bela R., Christiane Theda, Ali Fatemi, und Ann B. Moser. 2020. „X-linked Adrenoleukodystrophy: Pathology, Pathophysiology, Diagnostic Testing, Newborn

Screening and Therapies“. *International Journal of Developmental Neuroscience* 80 (1): 52–72. https://doi.org/10.1002/jdn.10003.
Van Den Bosch, Aletta M. R., Marlijn Van Der Poel, Nina L. Fransen, Maria C. J. Vincenten, Anneleen M. Bobeldijk, Aldo Jongejan, Hendrik J. Engelenburg, u. a. 2024. „Profiling of Microglia Nodules in Multiple Sclerosis Reveals Propensity for Lesion Formation“. *Nature Communications* 15 (1): 1667. https://doi.org/10.1038/s41467-024-46068-3.
Van Geel, B M, J Assies, E B Haverkort, J H T M Koelman, B Verbeeten, R J A Wanders, und P G Barth. 1999. „Progression of Abnormalities in Adrenomyeloneuropathy and Neurologically Asymptomatic X-Linked Adrenoleukodystrophy despite Treatment with ‚Lorenzo's Oil'“. *Journal of Neurology, Neurosurgery & Psychiatry* 67 (3): 290–99. https://doi.org/10.1136/jnnp.67.3.290.
VanRyzin, Jonathan W. 2021. „Phagocytic Microglia in Development: Are They What They Eat?“ *Brain, Behavior, & Immunity - Health* 18 (Dezember):100373. https://doi.org/10.1016/j.bbih.2021.100373.
Videbæk, Cecilie, Lars Melgaard, Allan M. Lund, und Sabine Weller Grønborg. 2023. „Newborn Screening for Adrenoleukodystrophy: International Experiences and Challenges“. *Molecular Genetics and Metabolism* 140 (4): 107734. https://doi.org/10.1016/j.ymgme.2023.107734.
Vilalta, Anna, und Guy C. Brown. 2018. „Neurophagy, the Phagocytosis of Live Neurons and Synapses by Glia, Contributes to Brain Development and Disease“. *The FEBS Journal* 285 (19): 3566–75. https://doi.org/10.1111/febs.14323.
Vogel, Andrea, Julia Stefanie Brunner, Alexander Hajto, Omar Sharif, und Gernot Schabbauer. 2022. „Lipid Scavenging Macrophages and Inflammation“. *Biochimica et Biophysica Acta (BBA) - Molecular and Cell Biology of Lipids* 1867 (1): 159066. https://doi.org/10.1016/j.bbalip.2021.159066.
Weber, F. D., C. Wiesinger, S. Forss-Petter, G. Regelsberger, A. Einwich, W. H. A. Weber, W. Kohler, H. Stockinger, und J. Berger. 2014. „X-Linked Adrenoleukodystrophy: Very Long-Chain Fatty Acid Metabolism Is Severely Impaired in Monocytes but Not in Lymphocytes“. *Human Molecular Genetics* 23 (10): 2542–50. https://doi.org/10.1093/hmg/ddt645.
Weinhofer, Isabelle, Bettina Zierfuss, Simon Hametner, Magdalena Wagner, Niko Popitsch, Christian Machacek, Barbara Bartolini, u. a. 2018. „Impaired Plasticity of Macrophages in X-Linked Adrenoleukodystrophy“. *Brain* 141 (8): 2329–42. https://doi.org/10.1093/brain/awy127.
Wirth, Thomas, Nigel Parker, und Seppo Ylä-Herttuala. 2013. „History of Gene Therapy“. *Gene* 525 (2): 162–69. https://doi.org/10.1016/j.gene.2013.03.137.
Wood, Heather B. 2010. „Successful Gene Therapy in X-Linked Adrenoleukodystrophy“. *Nature Reviews Neurology* 6 (1): 4–4. https://doi.org/10.1038/nrneurol.2009.204.
Yadav, Mangal Chandra, Bhavani Venkatachalam, Akshay Parmar, M. Aparna Krishnan, Reheema Thasli, und Sachchidanand Sinha. 2024. „Progressive Demyelinating Childhood Cerebral Adrenoleukodystrophy : Assessment of Communication Impairment“. *Rare* 2:100029. https://doi.org/10.1016/j.rare.2024.100029.
Yin, Kai, Duan-fang Liao, und Chao-ke Tang. 2010. „ATP-Binding Membrane Cassette Transporter A1 (ABCA1): A Possible Link between Inflammation and Reverse Cholesterol Transport“. *Molecular Medicine* 16 (9–10): 438–49. https://doi.org/10.2119/molmed.2010.00004.
Young, Alexander P., und Eileen M. Denovan-Wright. 2022. „The Dynamic Role of Microglia and the Endocannabinoid System in Neuroinflammation“. *Frontiers in Pharmacology* 12 (Februar):806417. https://doi.org/10.3389/fphar.2021.806417.
Zierfuss, Bettina, Agnieszka Buda, Andrea Villoria-González, Maxime Logist, Jure Fabjan, Patricia Parzer, Claire Battin, u. a. 2022. „Saturated Very Long-Chain Fatty Acids

Regulate Macrophage Plasticity and Invasiveness“. *Journal of Neuroinflammation* 19 (1): 305. https://doi.org/10.1186/s12974-022-02664-y.